

Unveiling the physical processes that regulate Galaxy Evolution with SPICA observations

Luigi Spinoglio – IAPS, INAF, Roma, Italy

SPICA Galaxy Evolution WG leader
SPICA/SAFARI Italian Responsible
Member of the SPICA Science Team of ESA



What are the hot science topics for SPICA in galaxy evolution?

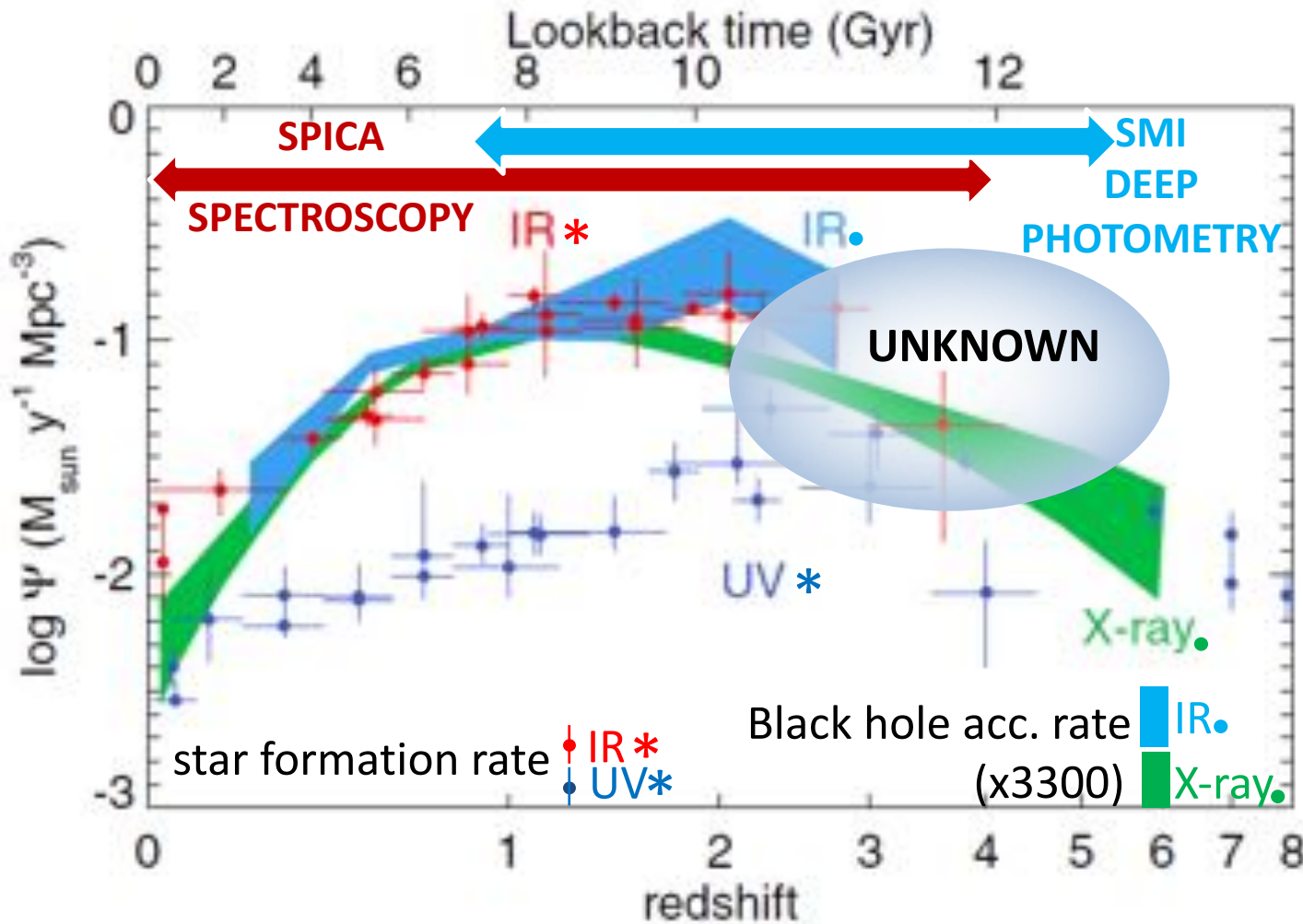
- Galaxy evolution case:

1. Mapping BHAR and SFR through spectroscopy at $0 < z < 4$
2. Feedback & Feeding in the context of galaxy evolution
3. Chemical Evolution of Galaxies: The Rise of Metals and Dust
4. Towards the epoch of Re-Ionization through photometric surveys
5. Towards the epoch of Re-Ionization through deep SAFARI spectroscopy

Explore:

SPICA-SMI $34\mu\text{m}$ +B-BOP $60\text{-}70\mu\text{m}$ (to be implemented) large-area deep surveys would provide 2-band continuum fluxes for unbiased samples of tens of thousands of galaxies

Galaxy evolution is obscured by dust at redshifts of $z \sim 1-3$



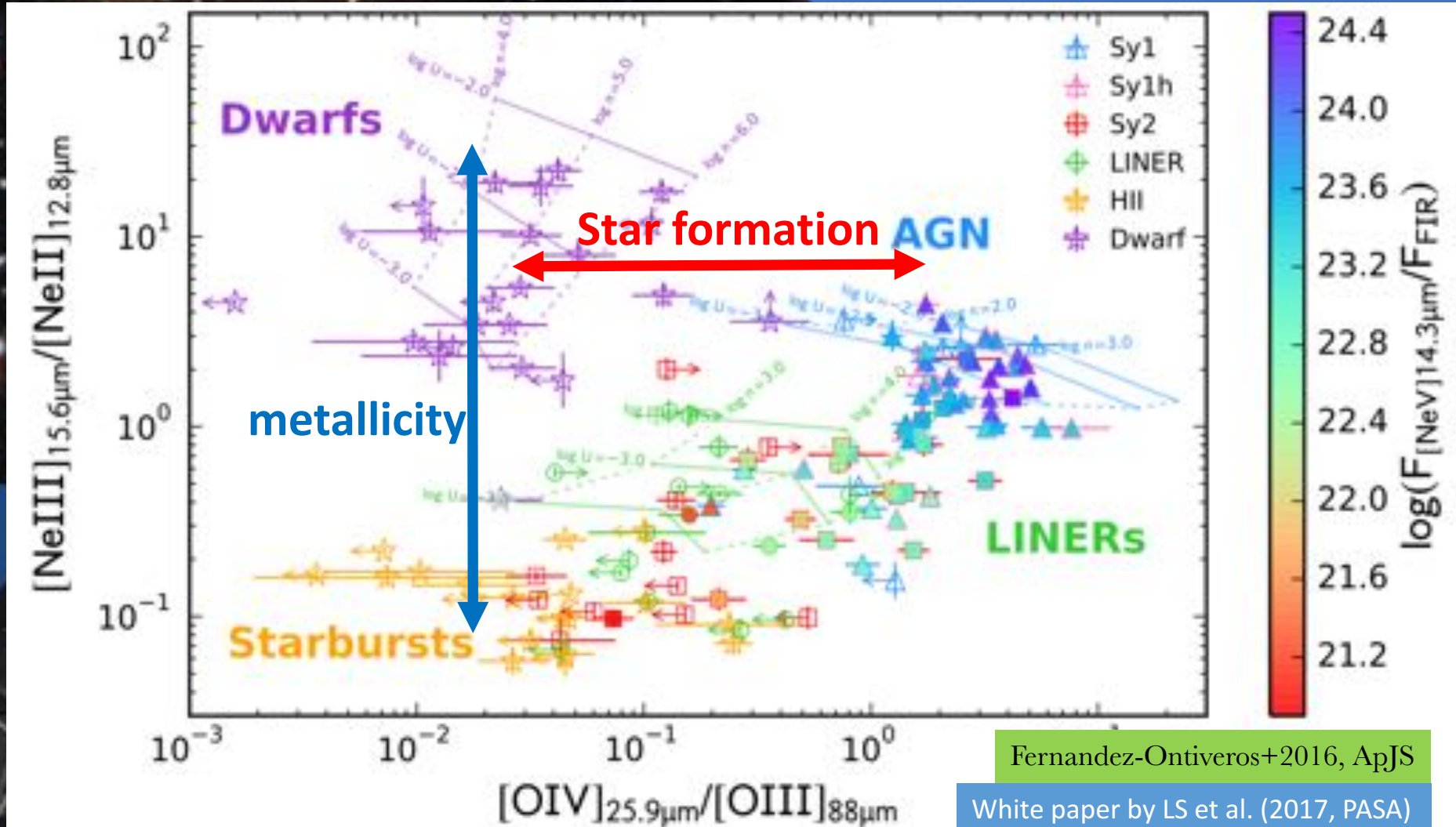
Spitzer + Herschel photometric surveys
 → bolometric luminosities of galaxies
 → estimates of the SFR and BHAR density functions.

However, AGN/SF separation is not based on observed physical quantities but is model-dependent (used local SED templates, with large uncertainty and degeneracy).

- UV/opt. spectroscopy (from e.g. SLOAN) track only marginally ($\sim 10\%$) the total integrated light.
- BHAR X-ray estimates are affected by the large uncertainties of the adopted bolometric corrections.
- SFR density at $z > 2-3$ very uncertain, since it is from UV surveys, highly affected by dust extinction.

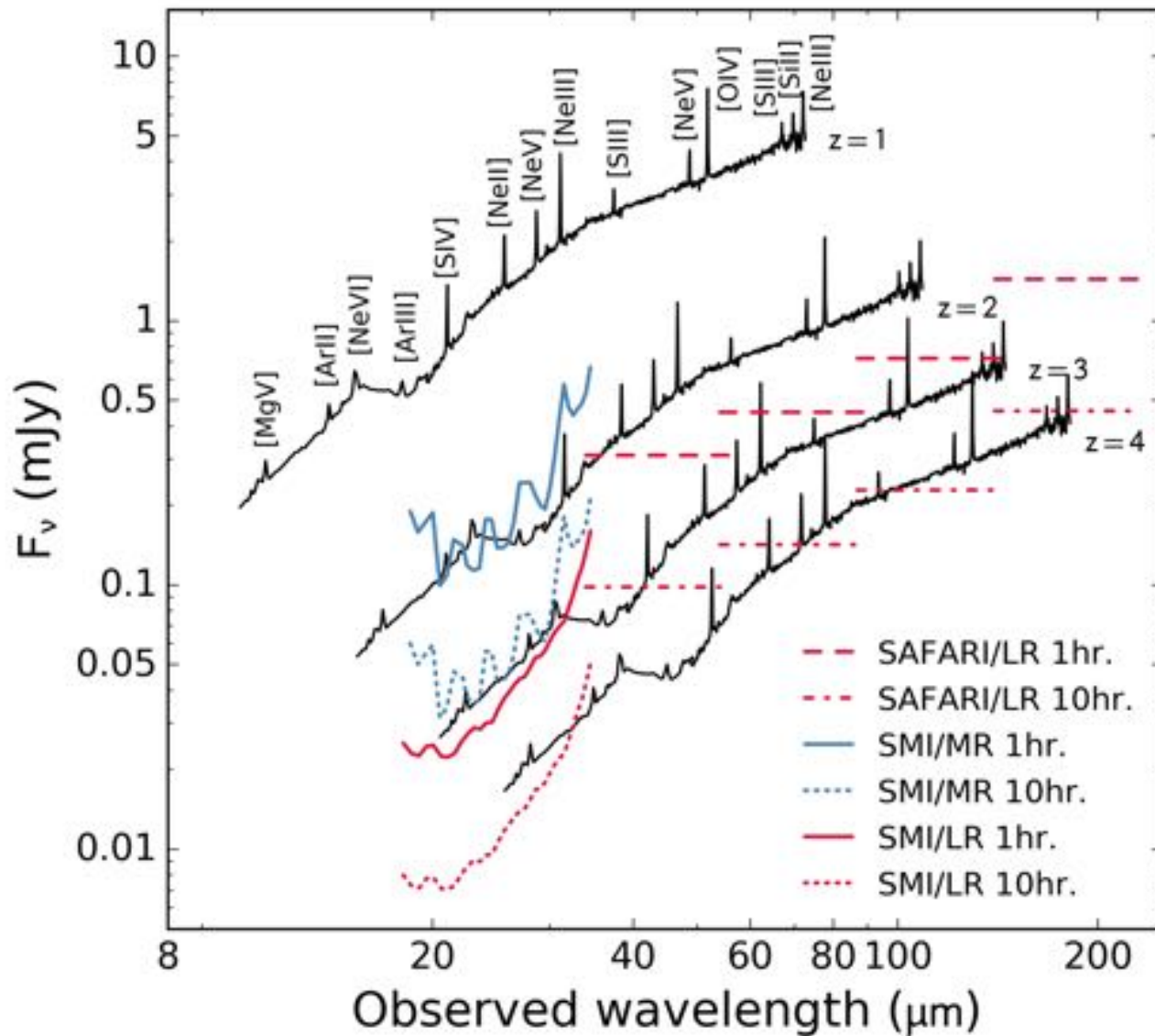
The new “IR BPT DIAGRAM”

SPICA will study both obscured starbursts and AGN across cosmic history, from a time when the Universe was only 1-2 billion years old.



- The new BPT diagram distinguishes any type of AGN (Seyfert and LINER) from any type of Star Formation dominated galaxy (either Starburst or Dwarf galaxies).

Line detectability with the SPICA spectrometers SAFARI & SMI



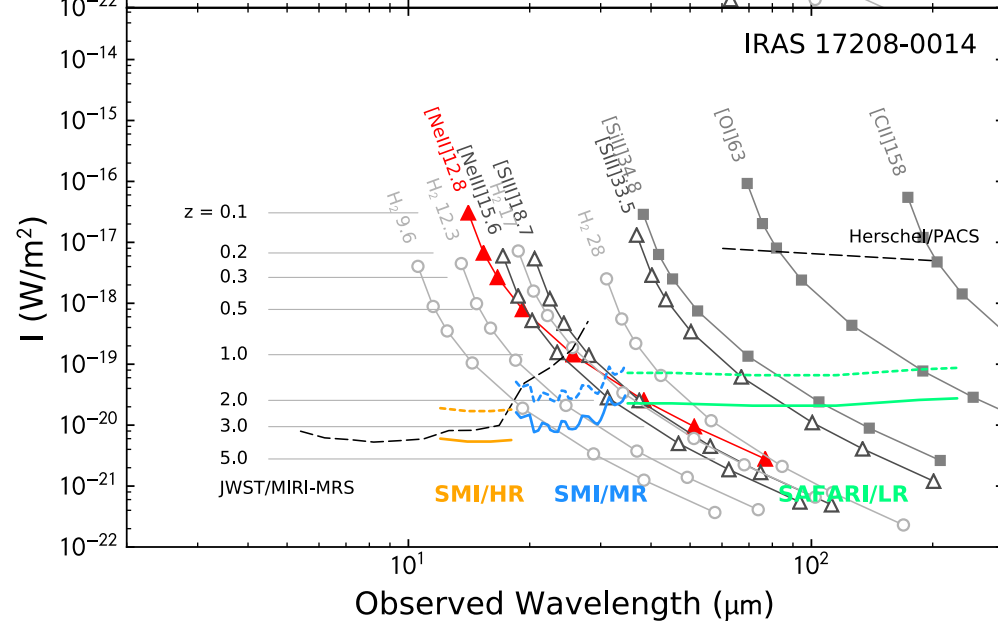
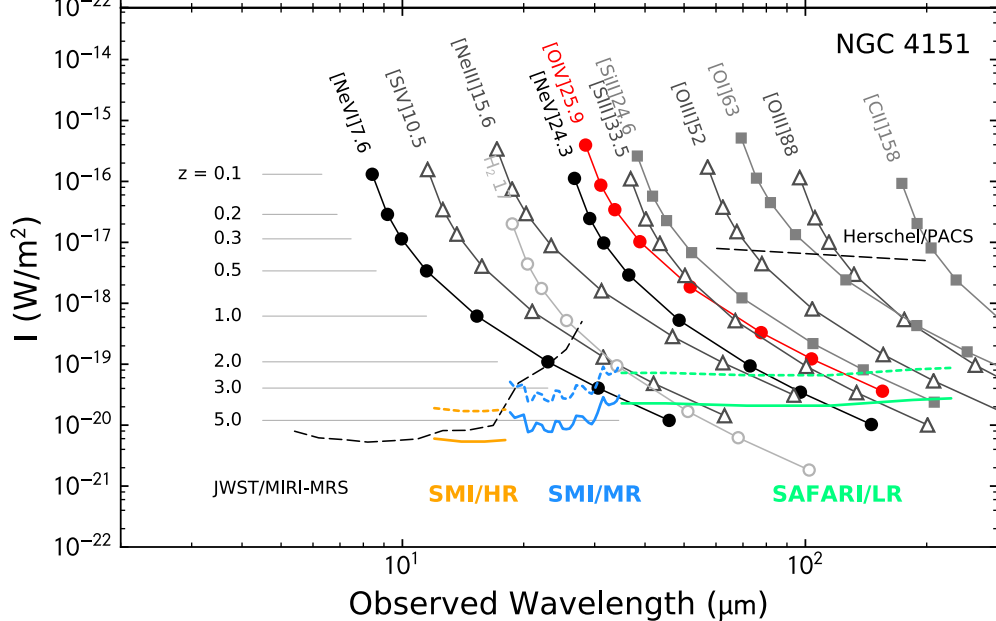
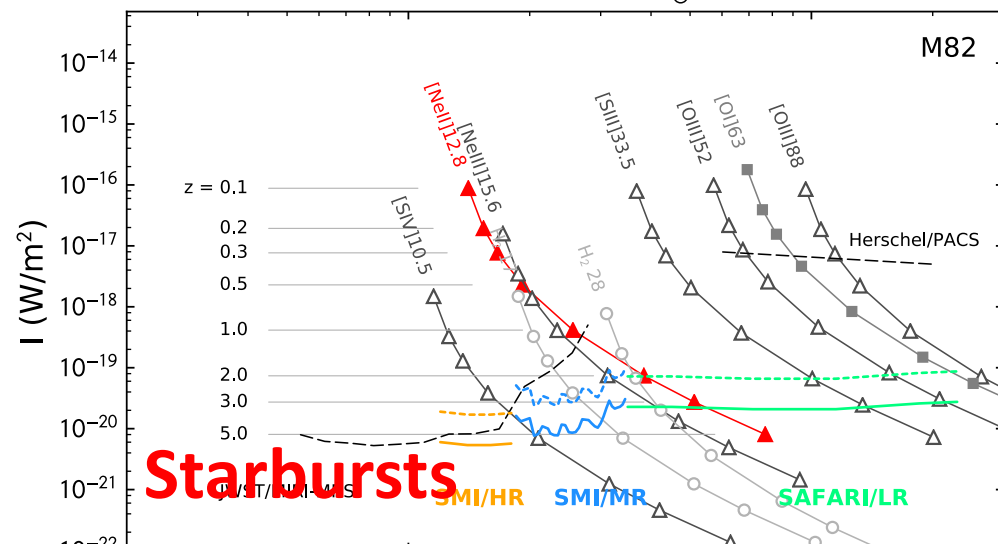
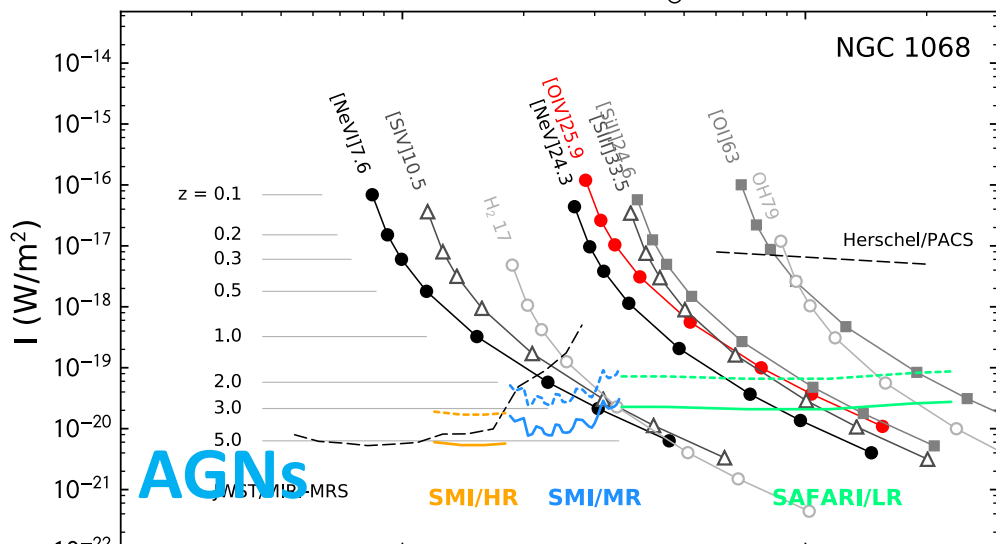
The IR spectrum of MCG-3-34-64, a nearby active galaxy, rescaled to a luminosity of $L=10^{12} L_\odot$ at redshifts z from 1 to 4. At $z=3$, the "main sequence luminosity" $L^*=10^{12} L_\odot$, implying that we will map the "bulk" of the galaxy population up to this redshift. The SAFARI and SMI sensitivities (in medium and low resolution) are shown.

White paper by LS et al. (2017, PASA)

Line detectability with the SPICA spectrometers SAFARI & SMI

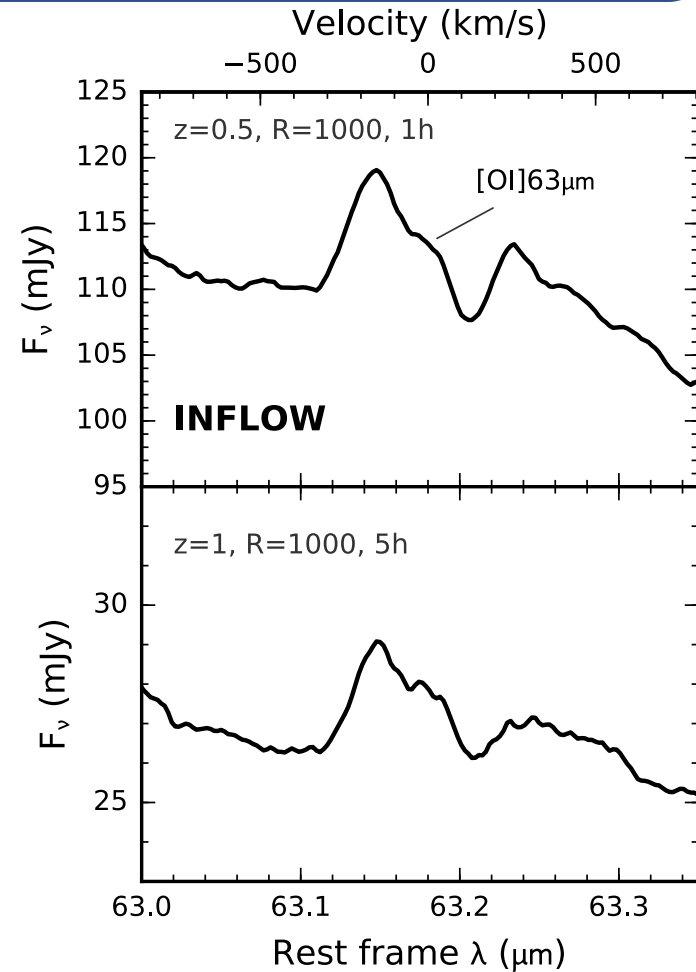
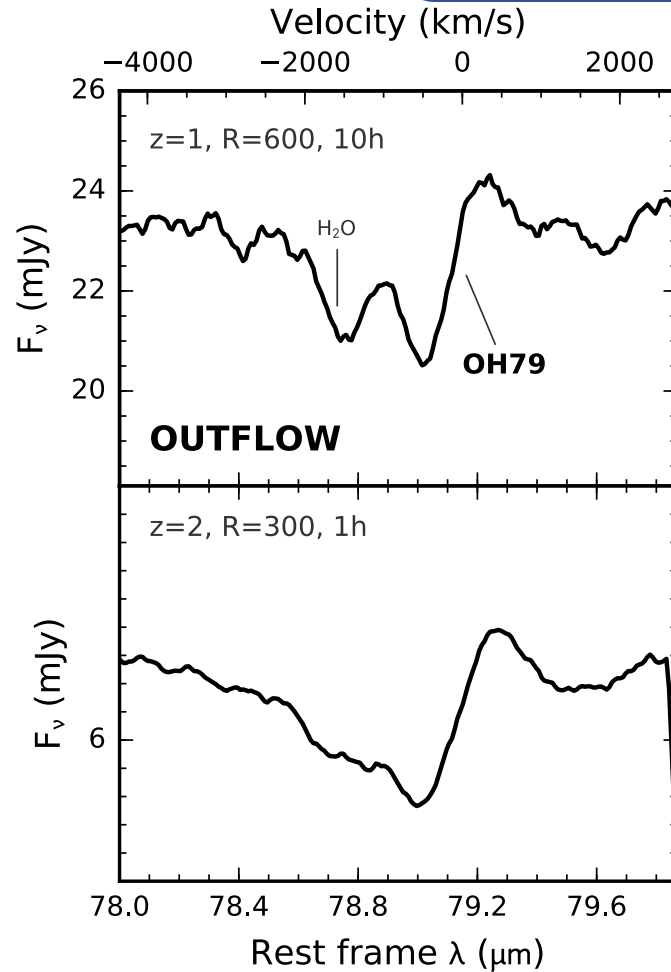
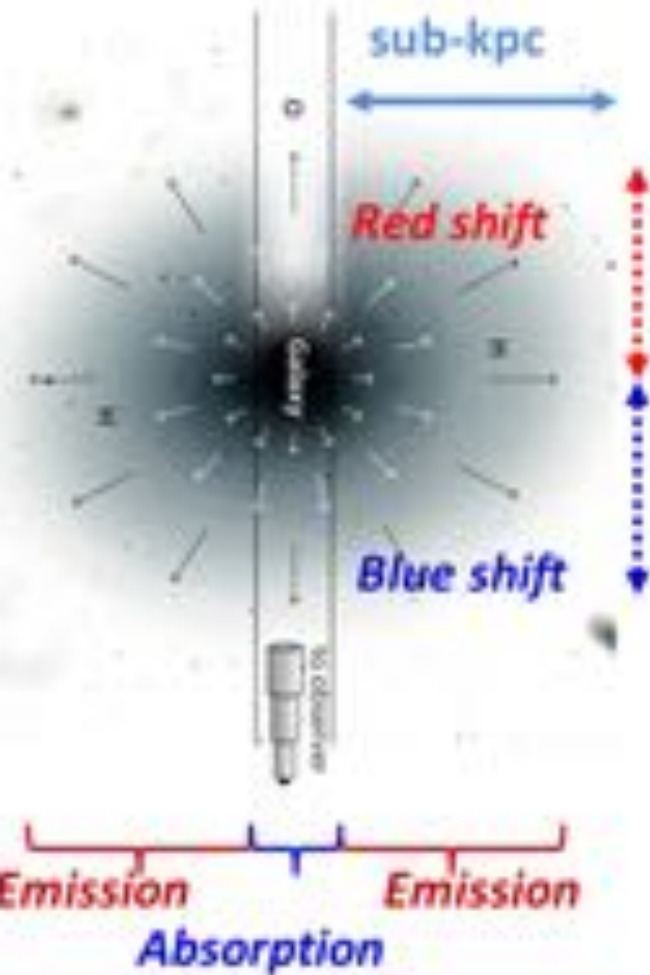
Scaled to $10^{12}L_{\odot}$

Scaled to $10^{12}L_{\odot}$



AGN feeding and feedback

SPICA will measure the key tracers of atomic and molecular outflows and infall in galaxies to the peak epoch of star formation



Left: Simulated SAFARI OH P-Cygni outflow spectra for a $L=2 \times 10^{12} L_\odot$ galaxy at $z=1$ and $z=2$, based on Herschel/PACS observations of Mrk231 (Gonzalez-Alfonso et al. 2014). Right: Simulated [OI]63 μm inverse P-Cygni inflow profile, based on PACS spectra of Zw049.057 (Falstad et al. 2015). SAFARI will detect outflow and inflow motions in ULIRGs up to $z \sim 1$.

Work provided by: Eduardo Gonzalez-Alfonso, Eckhard Sturm

Feedback & Feeding in the context of galaxy evolution

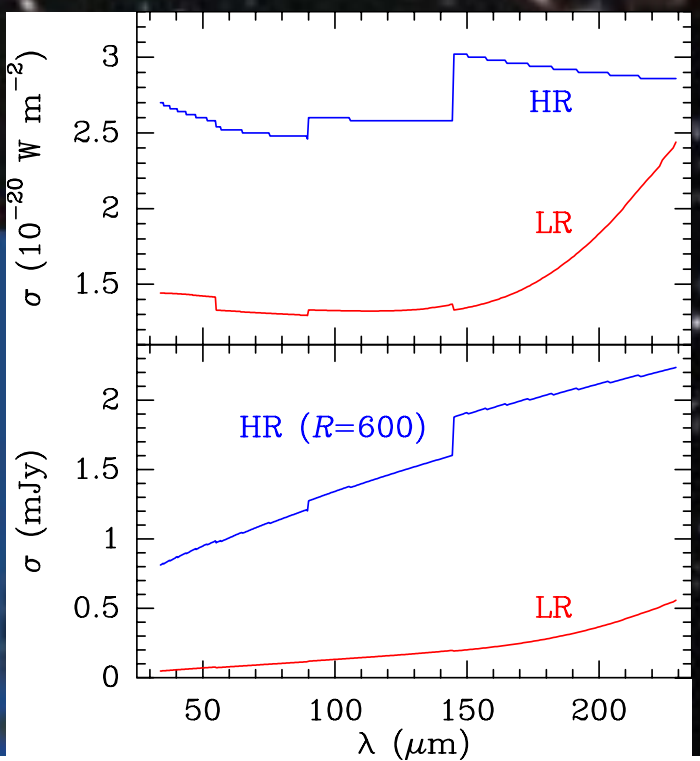
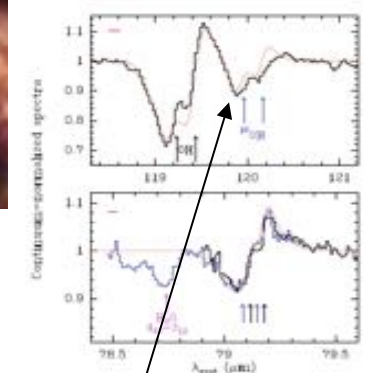
Does feedback stop star formation?

Low spectral resolution observations to measure statistics (outflow occurrence)

→ key tracers of atomic and molecular outflows/inflows in galaxies near the peak epoch of Star Formation ($z < 2$).

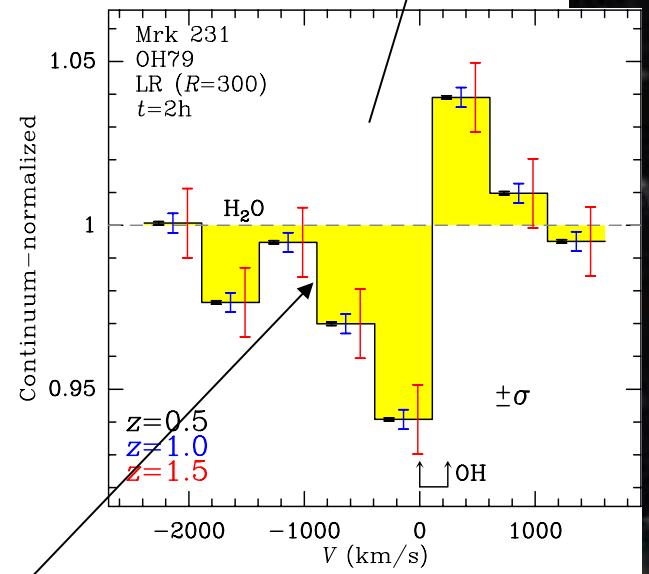
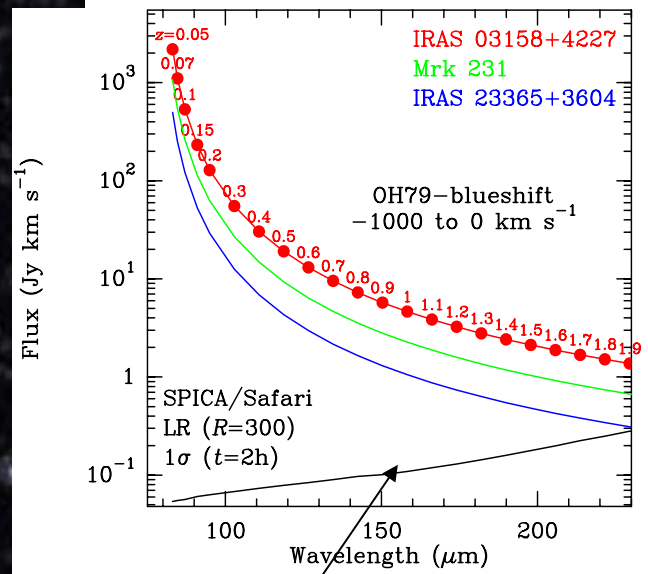
White paper by Eduardo González-Alfonso et al. (2017, PASA)

(P-Cygni OH profiles in Mrk 231; Fischer+2010)



Current SAFARI Low resolution (LR) and high-resolution (HR) sensitivities

The OH doublet at 79 μm can probe outflows up to $z \sim 1.4-1.9$



- *OH79 shows P-Cygni in many local ULIRGs
- *We use 3 templates: flux of blueshifted wings vs z
- *Black curve: Safari sensitivities in LR ($R=300$) mode
- *Continuum-normalized vs velocity is redshift-invariant
- *Errorbars: $\pm 1\sigma$ at $z=0.5, 1, 1.5$ (Mrk 231, LR-2h)

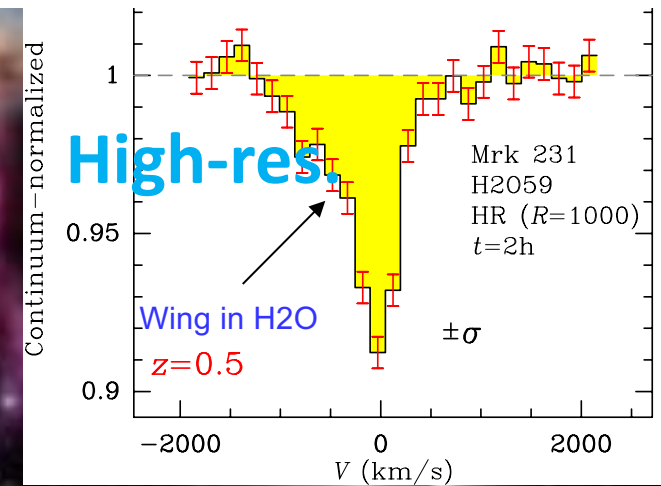
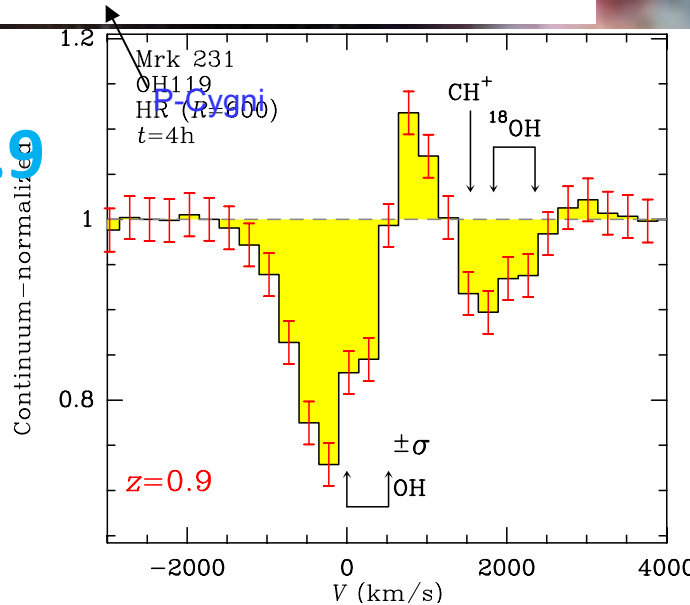
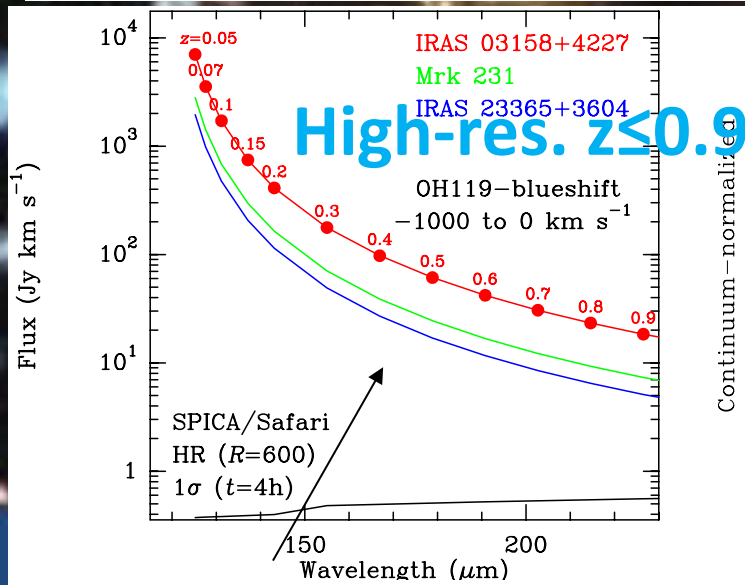
Low-res.
 $z \leq 1.9$

Feedback & Feeding in the context of galaxy evolution

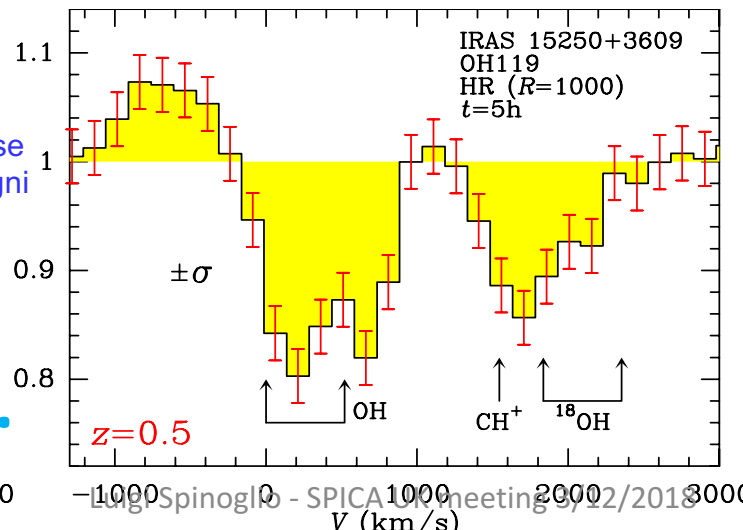
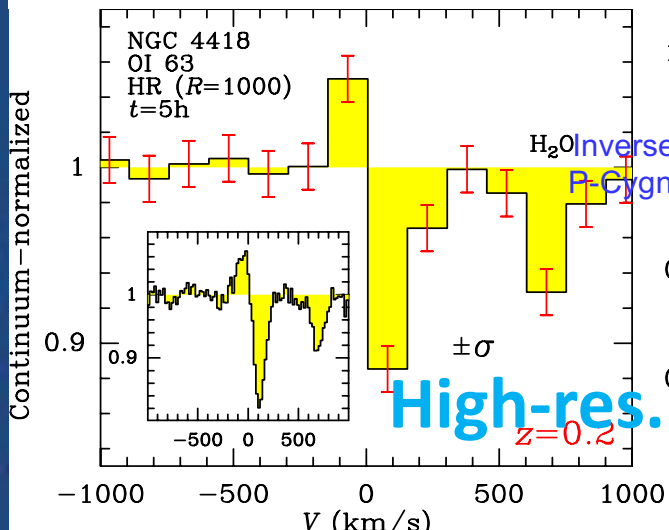
High spectral resolution observations to measure physical parameters (mass, energy, velocity...)

At high-R the OH doublet at 119 μm can be observed up to $z \sim 0.93$

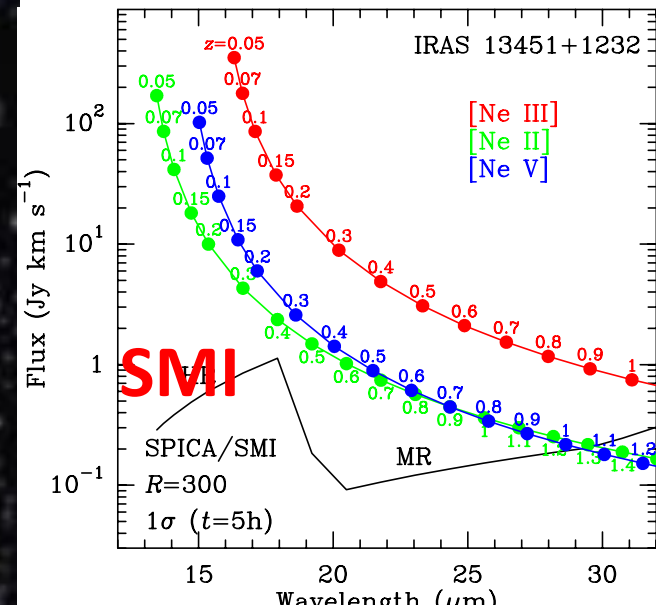
Outflows in other molecules, like H₂O



We will also explore inflows in [O I]63 μm and OH



SMI will detect outflows in Ne lines

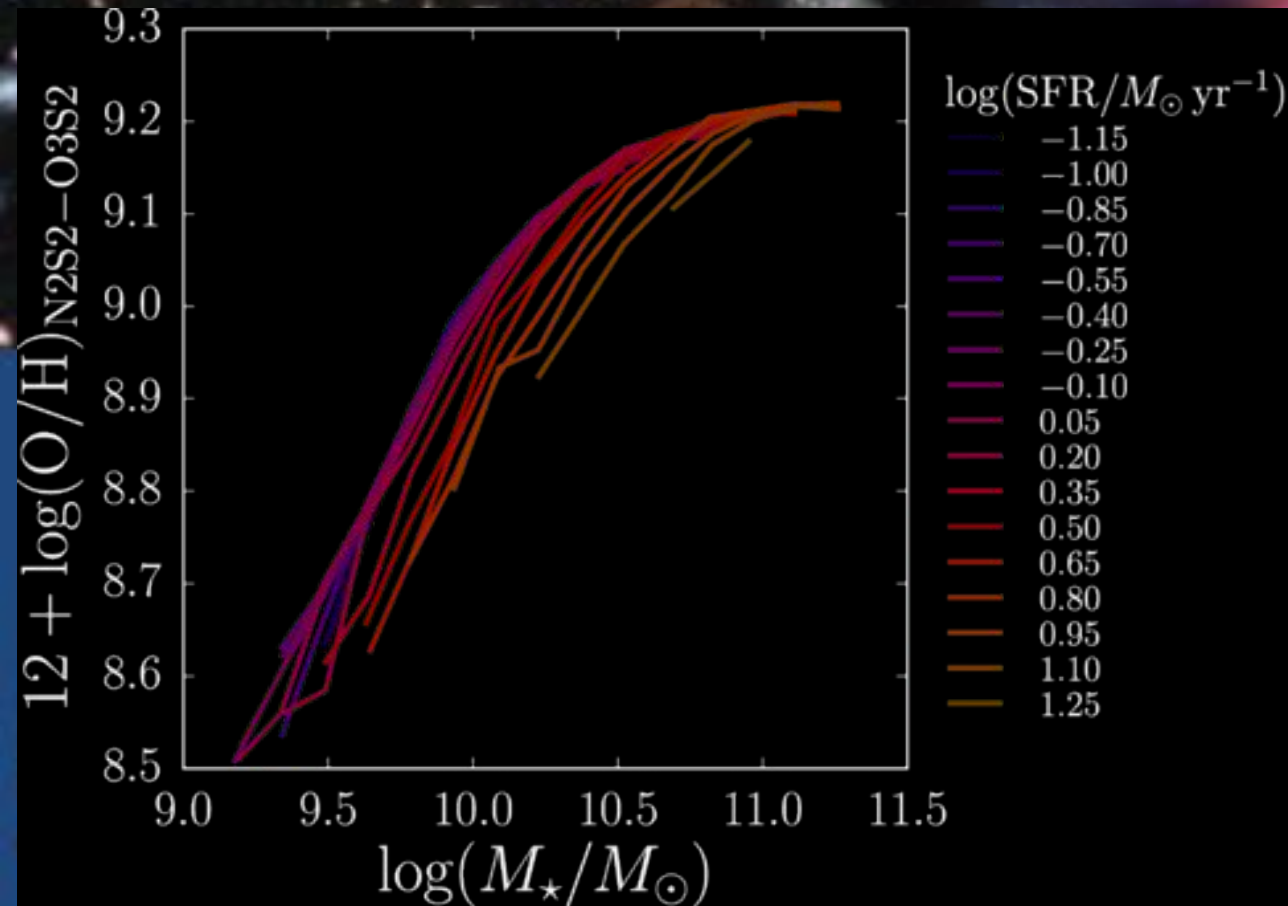


SPICA and the Chemical Evolution of Galaxies: The Rise of Metals and Dust

white paper by Juan Antonio Fernandez-Ontiveros et al. (2017, PASA)

Higher metallicities in massive galaxies (Lequeux+1979) in Local Universe

- Input for galaxy evolution models (Davé+2012,2017)
- Optical biased because of dust → IR tracers
- Optical tracers depend strongly on T_e



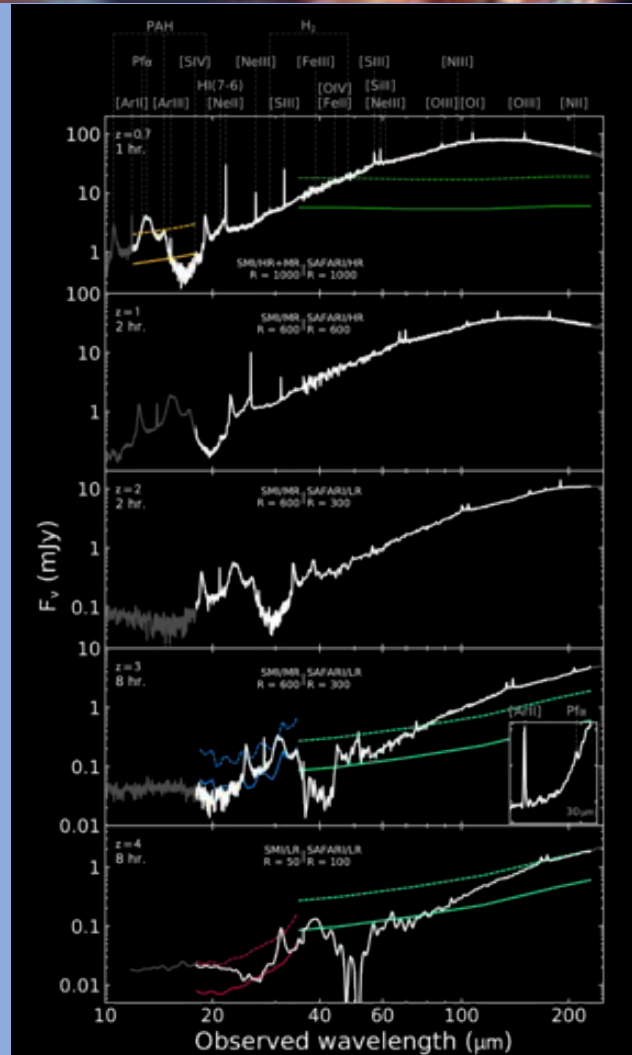
Measuring metallicities with SPICA IR lines

Direct method:

- Local Universe: Humphreys- α ($12.37 \mu\text{m}$)
- $1.5 < z < 3.0$: Pfund- α ($7.46 \mu\text{m}$)
- **Neon:**
[NeII] $12.8 \mu\text{m}$, [NeIII] $15.6 \mu\text{m}$
- **Sulphur:**
[SIV] $10.5 \mu\text{m}$, [SIII] $18.7 \mu\text{m}$
- **Argon:**
[ArII] $6.99 \mu\text{m}$, [ArIII] $8.99 \mu\text{m}$

Test this with JWST MIRI

SPICA: higher redshift



Measuring metallicities with SPICA IR lines

Indirect method:

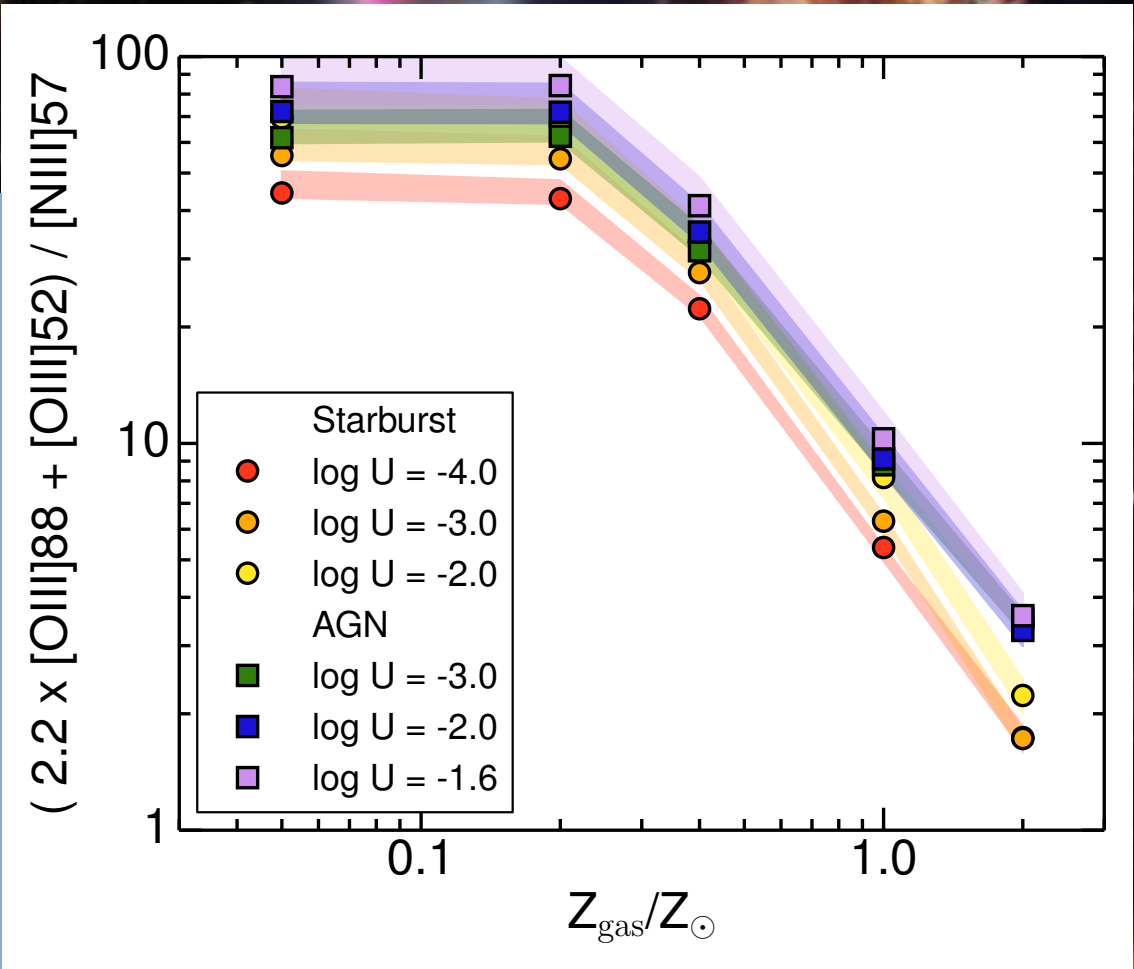
- Calibration is given by photoionization models (for AGN and starburst)

- $z < 1.6$

- Measure

$$\frac{2.2 \times [\text{Oiii}]_{88\mu\text{m}} + [\text{Oiii}]_{52\mu\text{m}}}{[\text{N iii}]_{57\mu\text{m}}}$$

(Nagao+2011 and Pereira- Santaella et al. 2017)

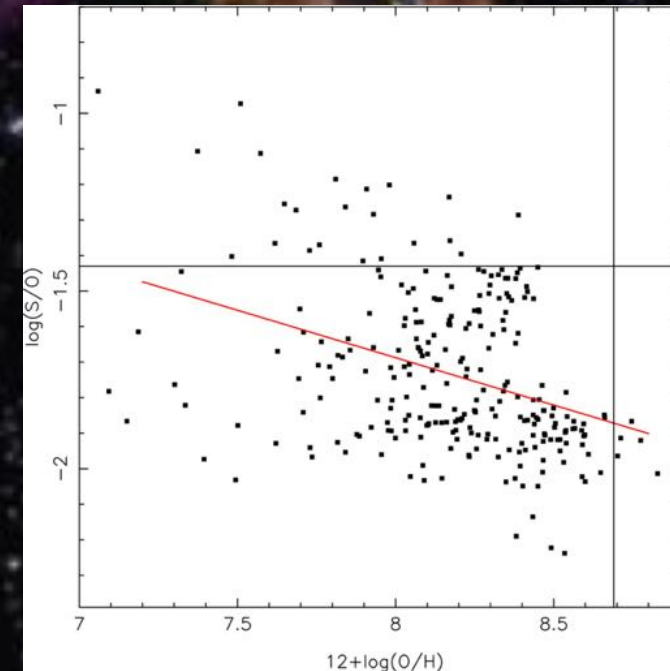
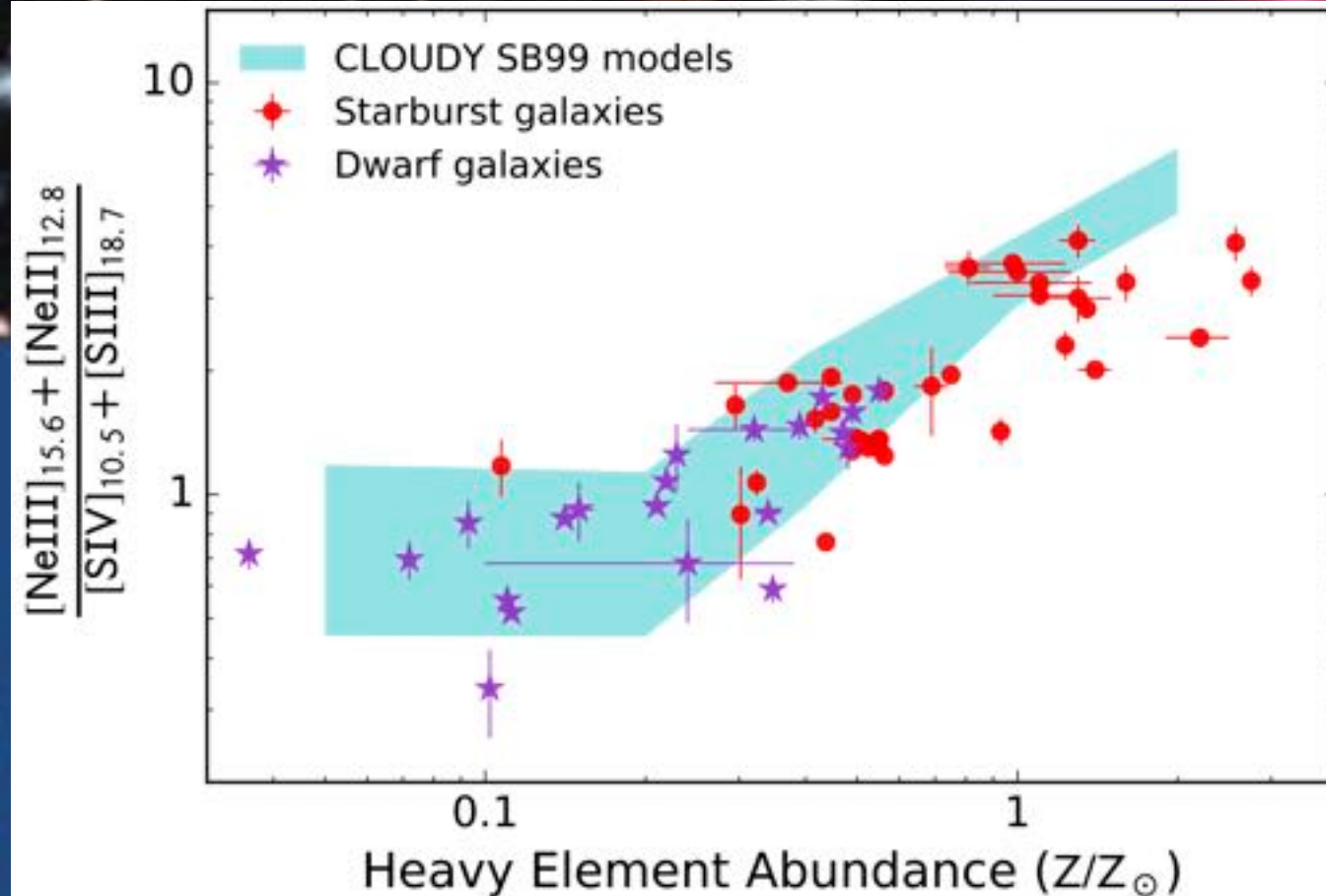


Measuring metallicities with SPICA IR lines

For $0.15 < z < 3$
measure:

$$\frac{[\text{NeII}]_{12.8\mu\text{m}} + [\text{NeIII}]_{15.6\mu\text{m}}}{[\text{SIII}]_{10.5\mu\text{m}} + [\text{SIV}]_{18.7\mu\text{m}}}$$

Spitzer /IRS observations of starburst galaxies in the Local Universe vs. indirect gas-phase optical metallicity (Moustakas et al. 2010; Pilyugin et al. 2014). Cloudy models including sulphur depletion above $Z > 1/5 Z_{\odot}$ are in agreement with the observations (adapted from Fernandez-Ontiveros et al. 2016).

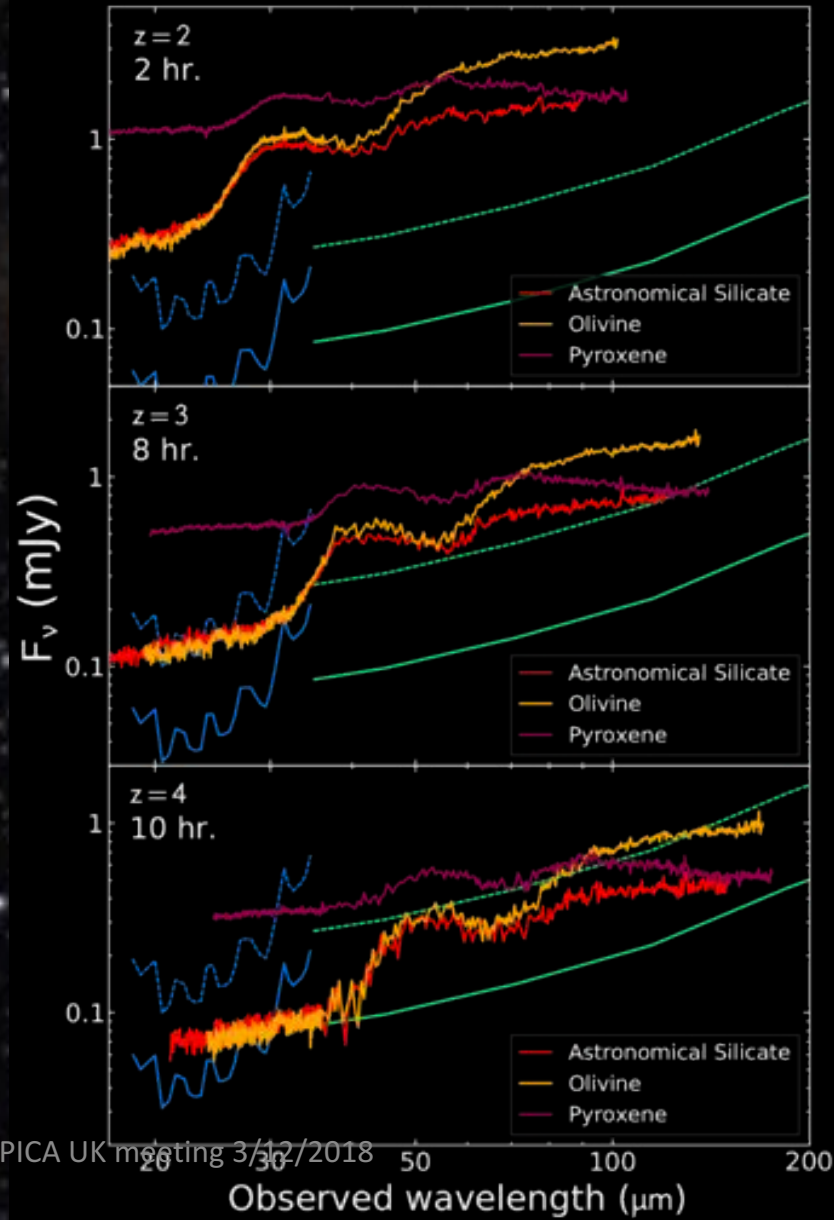


Measuring dust evolution with SPICA

- **Dust** ~1% ISM mass absorbs 30-50% of light
- **Origin and composition?**
- Condensation in **SNR** (Rho+2008)
- **Solid-state** features probe the **dust composition**

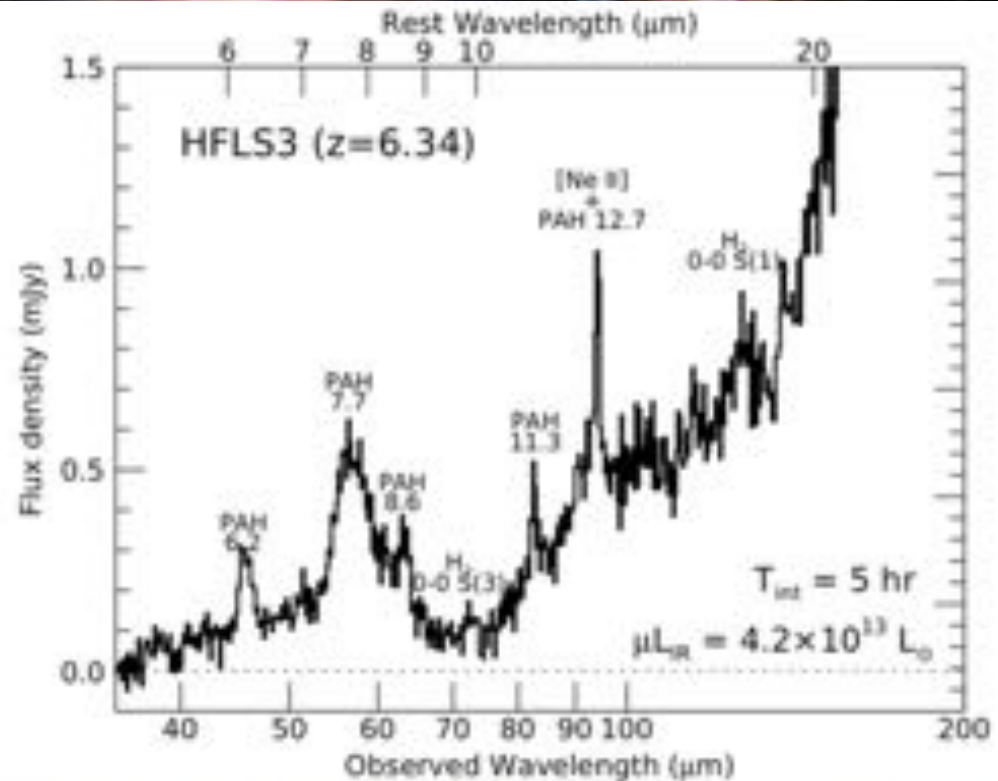
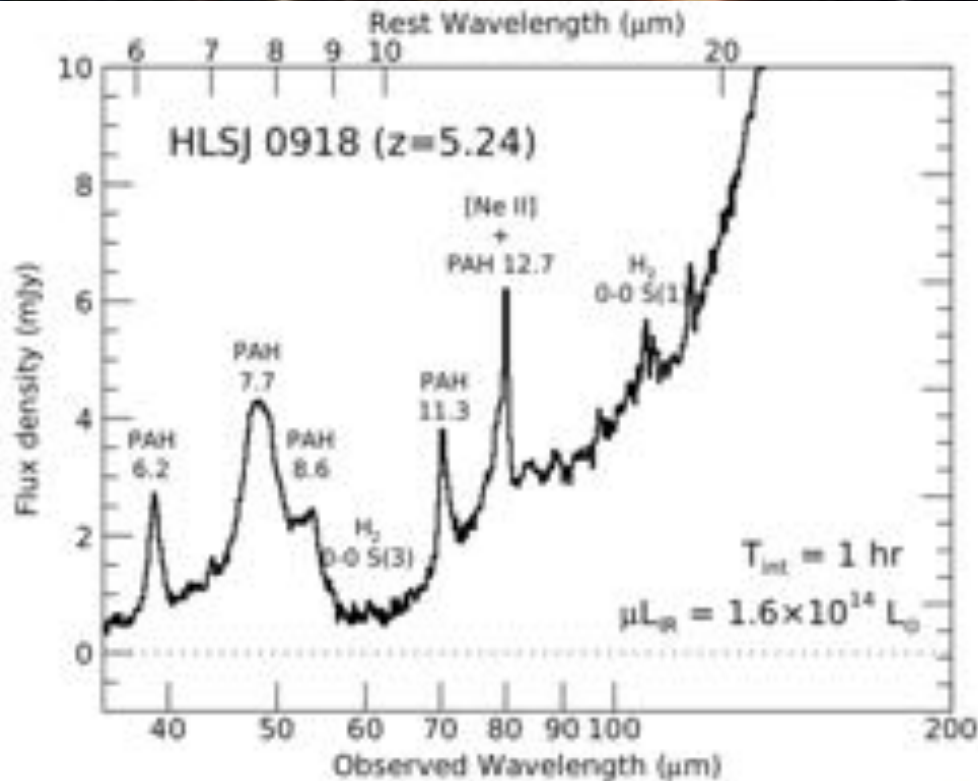
(Spoon+2006, Xie+2017)

white paper by Juan Antonio Fernandez-Ontiveros et al. (2017, PASA)



Probing the High-Redshift Universe with SPICA spectroscopy

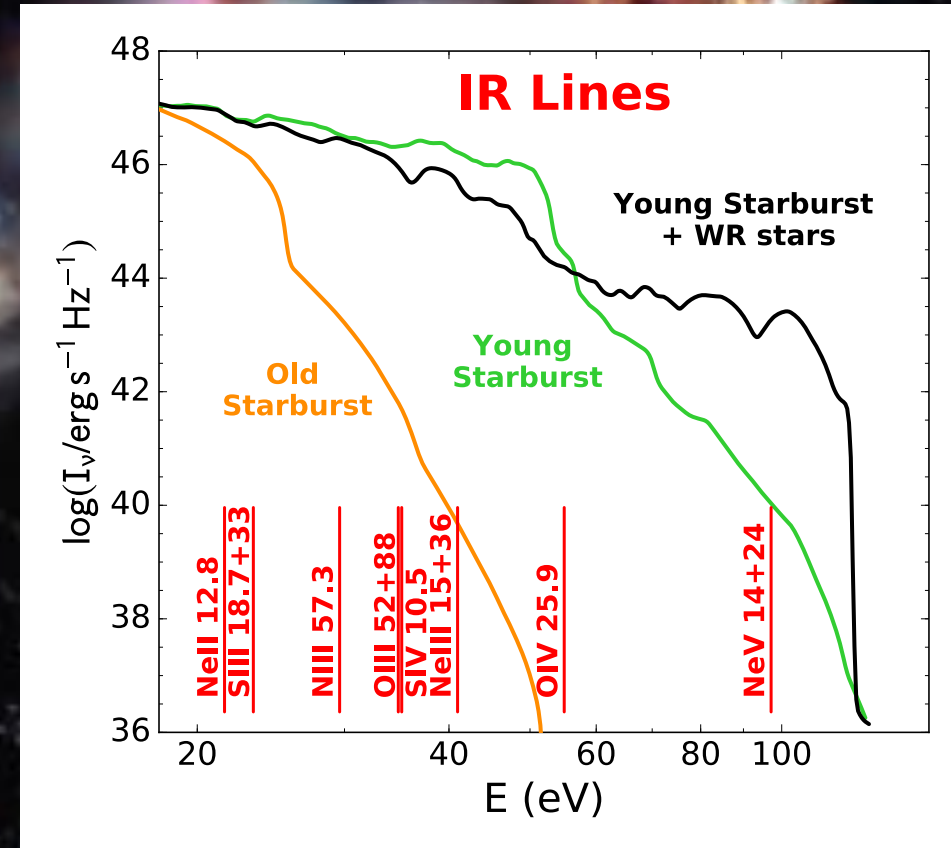
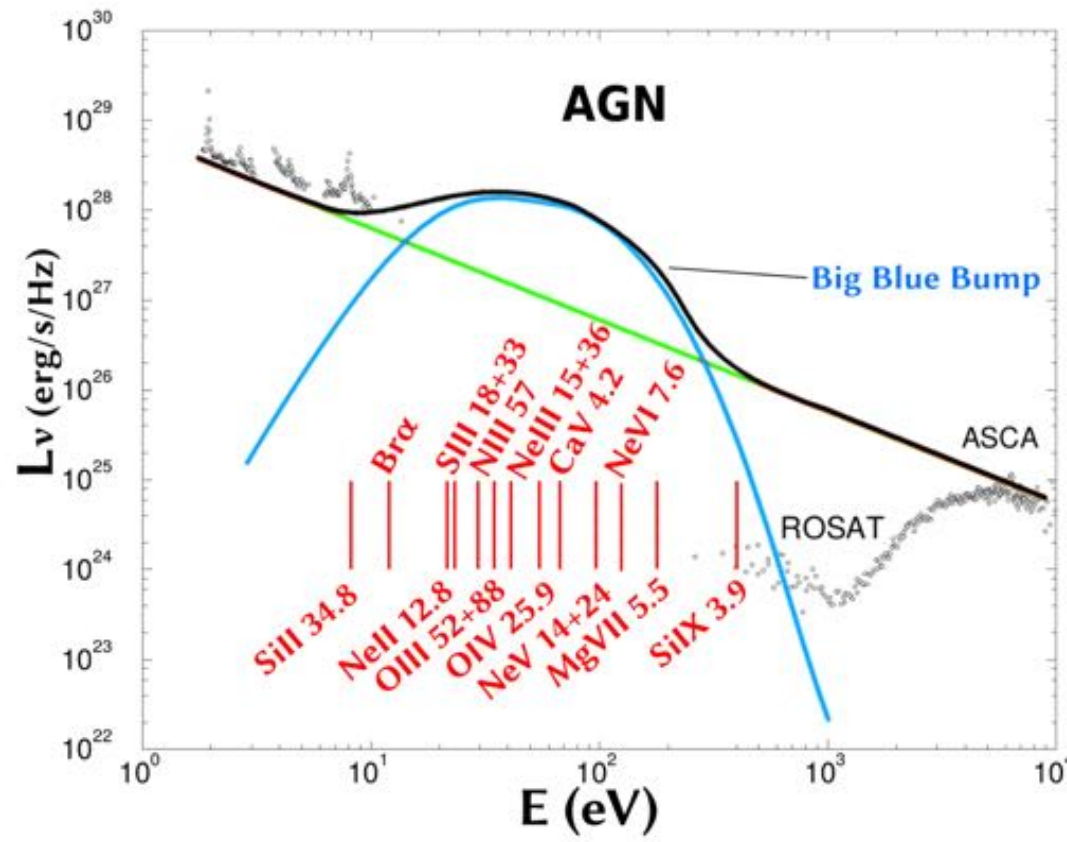
SAFARI will collect rest-frame mid-IR spectra up to $z \sim 10$ for sufficiently luminous galaxies ($L_{\text{IR}} > 2 \times 10^{13} L_{\odot}$). These galaxies, mostly gravitationally lensed, are being discovered at $z > 5$, (e.g. Combes et al. 2012; Riechers et al. 2013). SPICA will offer the first opportunity to study the rest-frame mid-IR spectra of galaxies at $z > 4-5$ and up to $z \sim 10$ in significant numbers.



Simulated SAFARI spectra of HLSJ0918 and HFLS3 produced with the $L_{\text{IR}} \sim 10^{12} L_{\odot}$ galaxy spectral template (Rieke et al. 2009), scaled to $\mu L_{\text{IR}} = 16$ and $4 \times 10^{13} L_{\odot}$, respectively. These are both gravitationally lensed by factors of 9 and 2, respectively.

Mapping the primary ionizing spectra of AGN and starburst galaxies

The IR fine structure lines are formed at ionization energies that can map the primary ionizing spectrum, where it is not observable because of absorption from our Galaxy.



Left: Overlay of the NGC4151 primary spectrum (black points) with a sketched “blue bump” and a power law (adapted from Alexander et al 1999). Right: A typical young and old starburst spectrum (models from Leitherer et al 1999). In both cases the key IR diagnostic lines are indicated. SPICA is a powerful probe of the invisible primary ionizing spectra of both AGN and starbursts.

From the science goals to the SPICA science requirements



How science requirements give the needed sensitivity for spectroscopy

Slice at z=1:

Log(L) (Lo)	F_o4 (W/m ²)	F_ne2 (W/m ²)	F_ne5 (W/m ²)
11.00	3.498e-20	3.406e-20	1.212e-20
11.50	9.649e-20	1.315e-19	3.742e-20
12.00	2.662e-19	5.077e-19	1.155e-19
12.50	7.343e-19	1.960e-18	3.567e-19
13.00	2.026e-18	7.567e-18	1.101e-18
13.50	5.588e-18	2.922e-17	3.400e-18

Slice at z=2:

Log(L) (Lo)	F_o4 (W/m ²)	F_ne2 (W/m ²)	F_ne5 (W/m ²)
11.50	1.732e-20	2.360e-20	6.715e-21
12.00	4.777e-20	9.111e-20	2.073e-20
12.50	1.318e-19	3.518e-19	6.401e-20
13.00	3.635e-19	1.358e-18	1.976e-19
13.50	1.003e-18	5.243e-18	6.102e-19

Slice at z=3:

Log(L) (Lo)	F_o4 (W/m ²)	F_ne2 (W/m ²)	F_ne5 (W/m ²)
12.00	1.777e-20	3.390e-20	7.714e-21
12.50	4.903e-20	1.309e-19	2.381e-20
13.00	1.353e-19	5.053e-19	7.353e-20
13.50	3.731e-19	1.951e-18	2.270e-19

The case is very simple:

We want to measure the bulk of the Star Formation Rate (SFR) and of the Black Hole Accretion Rate (BHAR) through cosmic time up to the peak of these functions i.e. at redshift of z=3.

To do this we need to detect the chosen tracers (namely the [OIV]26 μ m line for BHAR and the [NeII]12.8 μ m line for SFR) in the “typical” galaxies which produce most of the emission, i.e. the galaxies lying at the knee of the luminosity functions, at the three chosen redshifts of z=1, 2, 3, which also corresponds to the so-called “main sequence galaxies”.

We therefore adopt as limiting luminosity the “main-sequence” luminosity (in light blue)

We list in the table the expected fluxes of these galaxies at the various redshifts and luminosities.

BASELINE SPECTROSCOPIC SURVEYS (5×10^{-20} W/m² 5σ 1 hr.)

Slice at $z=1$: [NOTE: MIN. OBSERVING TIME on-source SET TO 0.1 hrs.]

Log(L)	F_o4	time_o4	F_ne2	time_ne2	F_ne5	time_ne5	adopted time
11.00	3.498e-20	2.044	3.406e-20	2.155	(1.212e-20)	17.02)	2 hrs.
11.50	9.649e-20	0.269	1.315e-19	0.145	3.742e-20	1.786	2 hrs.
12.00	2.662e-19	0.035	5.077e-19	0.010	1.155e-19	0.187	0.25 hrs.
12.50	7.343e-19	0.005	1.960e-18	0.001	3.567e-19	0.020	0.25 hrs.
13.00	2.026e-18	0.001	7.567e-18	0.000	1.101e-18	0.002	0.1 hrs.
13.50	5.588e-18	0.000	2.922e-17	0.000	3.400e-18	0.000	0.1 hrs.

total time for $z=1$ bin = $\sum_{L_{\text{bin}}=1,6} (\text{time}) \times 60$ sources = 4.7 x 60 sources = 282 hours

Slice at $z=2$:

Log(L)	F_o4	time_o4	F_ne2	time_ne2	F_ne5	time_ne5	adopted time
11.50	1.732e-20	8.337	2.360e-20	4.489	(6.715e-21)	55.4)	8 hrs.
12.00	4.777e-20	1.096	9.111e-20	0.301	2.073e-20	5.82	6 hrs.
12.50	1.318e-19	0.144	3.518e-19	0.020	6.401e-20	0.610	1 hr.
13.00	3.635e-19	0.019	1.358e-18	0.001	1.976e-19	0.064	0.5 hr.
13.50	1.003e-18	0.002	5.243e-18	0.000	6.102e-19	0.007	0.25 hr.

total time for $z=2$ bin = $\sum_{L_{\text{bin}}=1,5} (\text{time}) \times 60$ sources = 15.75 x 60 sources = 945 hours

Slice at $z=3$:

Log(L)	F_o4	time_o4	F_ne2	time_ne2	F_ne5	time_ne5	adopted time
12.00	1.777e-20	7.914	3.390e-20	2.176	(7.714e-21)	42.01)	8 hrs.
12.50	4.903e-20	1.040	1.309e-19	0.146	2.381e-20	4.41	4.5 hrs.
13.00	1.353e-19	0.137	5.053e-19	0.010	7.353e-20	0.462	0.5 hrs.
13.50	3.731e-19	0.018	1.951e-18	0.001	2.270e-19	0.049	0.5 hrs.

total time for $z=3$ bin = $\sum_{L_{\text{bin}}=1,4} (\text{time}) \times 60$ sources = 13.5 x 60 sources = 810 hours

Total Observing time on-source (without overheads) = 2040 hours for 900 sources

GOAL SPECTROSCOPIC SURVEYS (3×10^{-20} W/m² 5σ 1 hr.)

Slice at $z=1$: [NOTE: MIN. OBSERVING TIME on-source SET TO 0.1 hrs.]

Log(L)	F_o4	time_o4	F_ne2	time_ne2	F_ne5	time_ne5	adopted time
11.00	3.498e-20	0.735	3.406e-20	0.775	(1.212e-20)	6.126)	0.8 hrs.
11.50	9.649e-20	0.097	1.315e-19	0.052	3.742e-20	0.643	0.6 hrs.
12.00	2.662e-19	0.013	5.077e-19	0.003	1.155e-19	0.067	0.1 hrs.
12.50	7.343e-19	0.002	1.960e-18	0.000	3.567e-19	0.007	0.1 hrs.
13.00	2.026e-18	0.000	7.567e-18	0.000	1.101e-18	0.000	0.1 hrs.
13.50	5.588e-18	0.000	2.922e-17	0.000	3.400e-18	0.000	0.1 hrs.

total time for $z=1$ bin = $\sum_{L_{bin}=1,6}$ (time) x 60 sources = 1.80 x 60 sources = 108 hours

Slice at $z=2$:

Log(L)	F_o4	time_o4	F_ne2	time_ne2	F_ne5	time_ne5	adopted time
11.50	1.732e-20	3.000	2.360e-20	1.616	(6.715e-21)	19.9)	3 hrs.
12.00	4.777e-20	0.394	9.111e-20	0.108	2.073e-20	2.094	2 hrs.
12.50	1.318e-19	0.052	3.518e-19	0.007	6.401e-20	0.220	0.3 hr.
13.00	3.635e-19	0.007	1.358e-18	0.000	1.976e-19	0.023	0.1 hr.
13.50	1.003e-18	0.001	5.243e-18	0.000	6.102e-19	0.002	0.1 hr.

total time for $z=2$ bin = $\sum_{L_{bin}=1,5}$ (time) x 60 sources = 5.5 x 60 sources = 330 hours

Slice at $z=3$:

Log(L)	F_o4	time_o4	F_ne2	time_ne2	F_ne5	time_ne5	adopted time
12.00	1.777e-20	2.850	3.390e-20	0.783	(7.714e-21)	15.12)	3.6 hrs.
12.50	4.903e-20	0.374	1.309e-19	0.052	2.381e-20	1.587	2.0 hrs.
13.00	1.353e-19	0.049	5.053e-19	0.004	7.353e-20	0.166	0.22 hrs.
13.50	3.731e-19	0.006	1.951e-18	0.000	2.270e-19	0.017	0.1 hrs.

total time for $z=3$ bin = $\sum_{L_{bin}=1,4}$ (time) x 60 sources = 5.84 x 60 sources = 355 hours

Total Observing time on-source (without overheads) = **760 hours for 900 sources**

Summary science requirements: needed sensitivity for spectroscopy

[OIV] line fluxes as a function of z and Luminosity	Grating + 2.5m tel NEP=2x10 ⁻¹⁹ W/vHz	Grating + elliptical tel. 3m equivalent NEP=2x10 ⁻¹⁹ W/vHz or 2.5m tel + det. NEP ≤ 1.4x10 ⁻¹⁹ W/vHz	Grating + elliptical tel. 3m equivalent NEP=2x10 ⁻¹⁹ W/vHz or 2.5m tel + det. NEP ~ 1.0x10 ⁻¹⁹ W/vHz
Line sensitivity 5 sigma 1 hour (W/m ²)	7.2E-20 current	5.0E-20 requirement	3.0E-20 goal
	Max int.t./source Total survey time	Max int.t./source Total survey time	Max int.t./source Total survey time
z=1, L≥10 ¹¹ Lo 360 sources	4.2 hours 510 hours	2 hours 282 hours	0.8 hours 108 hours
z=2, L≥10 ^{11.5} Lo 300 sources	16.3 hours 1764 hours	8 hours 945 hours	3.0 hours 330 hours
z=3, L≥10 ¹² Lo 240 sources	15.5 hours 1506 hours	8 hours 810 hours	3.6 hours 355 hours
TOTAL SURVEY TIME	3780 hours	2037 hours	793 hours

Summary science requirements: needed spectral resolution

For most galaxy evolution observations:

1. Mapping BHAR and SFR through spectroscopy at $0 < z < 4$
2. Chemical Evolution of Galaxies: The Rise of Metals and Dust
3. Towards the epoch of Re-ionization through deep SAFARI spectroscopy

the required spectral resolution was set to $R=500$, [able to e.g. separate the [FeII] from the [OIV] fine structure lines at $26\mu\text{m}$] however for instrumental constraints it was relaxed to $R=300$ which is the current baseline for SAFARI

SMI low resolution spectroscopic images ($R=50-120$) will be adequate for the dust and PAH features and the slope of the MIR continuum, while the medium resolution spectrometer ($R=1300-2300$) will be used to extend the domain of the spectroscopic surveys to lower wavelengths.

However, the observations related to:

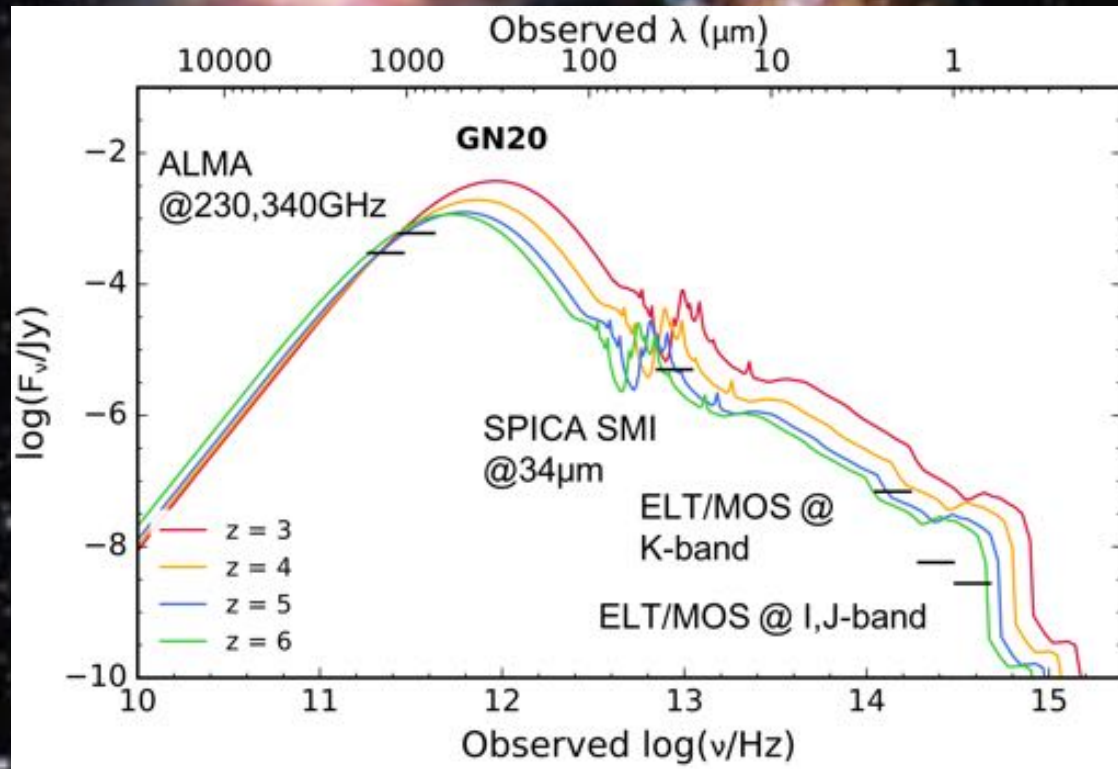
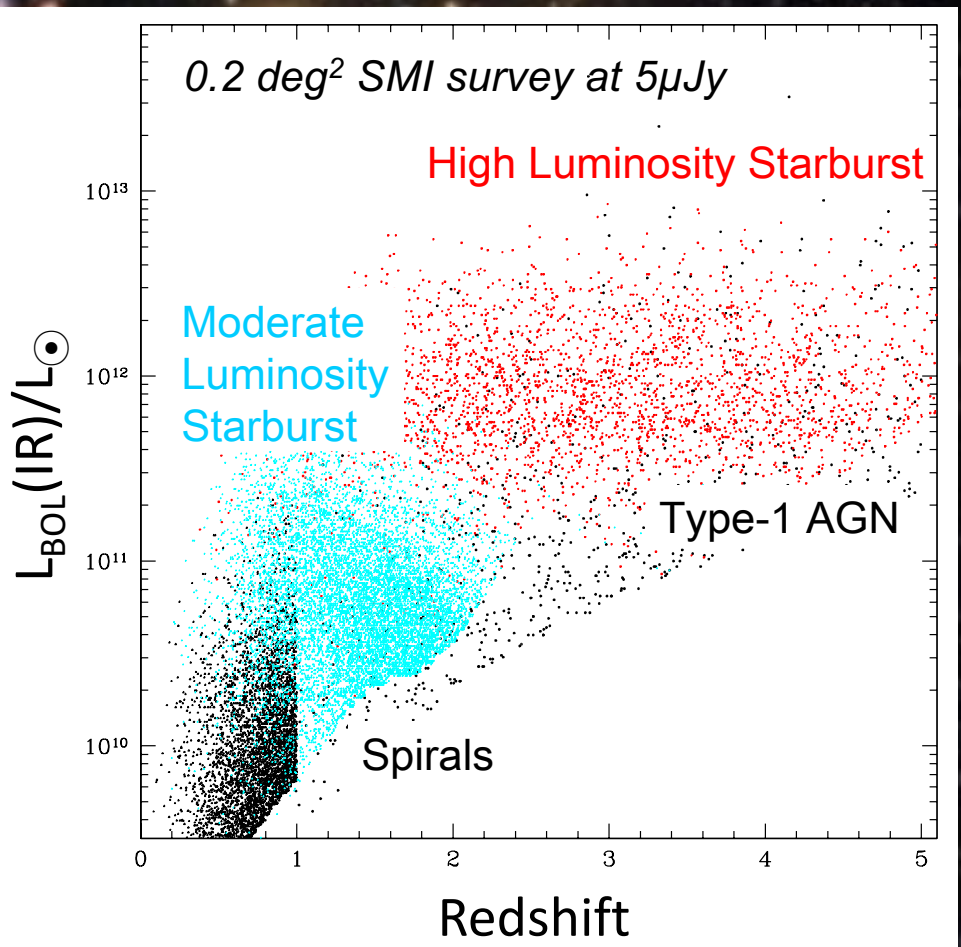
4. Feedback & Feeding in the context of galaxy evolution

does need high resolution spectra of at least that of the PACS spectrometer. The Martin-Puplett resolution ranges from 2000 to 12000 as inverse function of wavelength (from 35 to $230\mu\text{m}$) will be used together with the SMI medium resolution spectrometer ($R=1300-2300$). The SMI high resolution channel at $12-18\mu\text{m}$ might be used for profiles exploration.

SPICA PHOTOMETRIC SURVEYS

Towards the epoch of Re-ionization: early black holes and starbursts

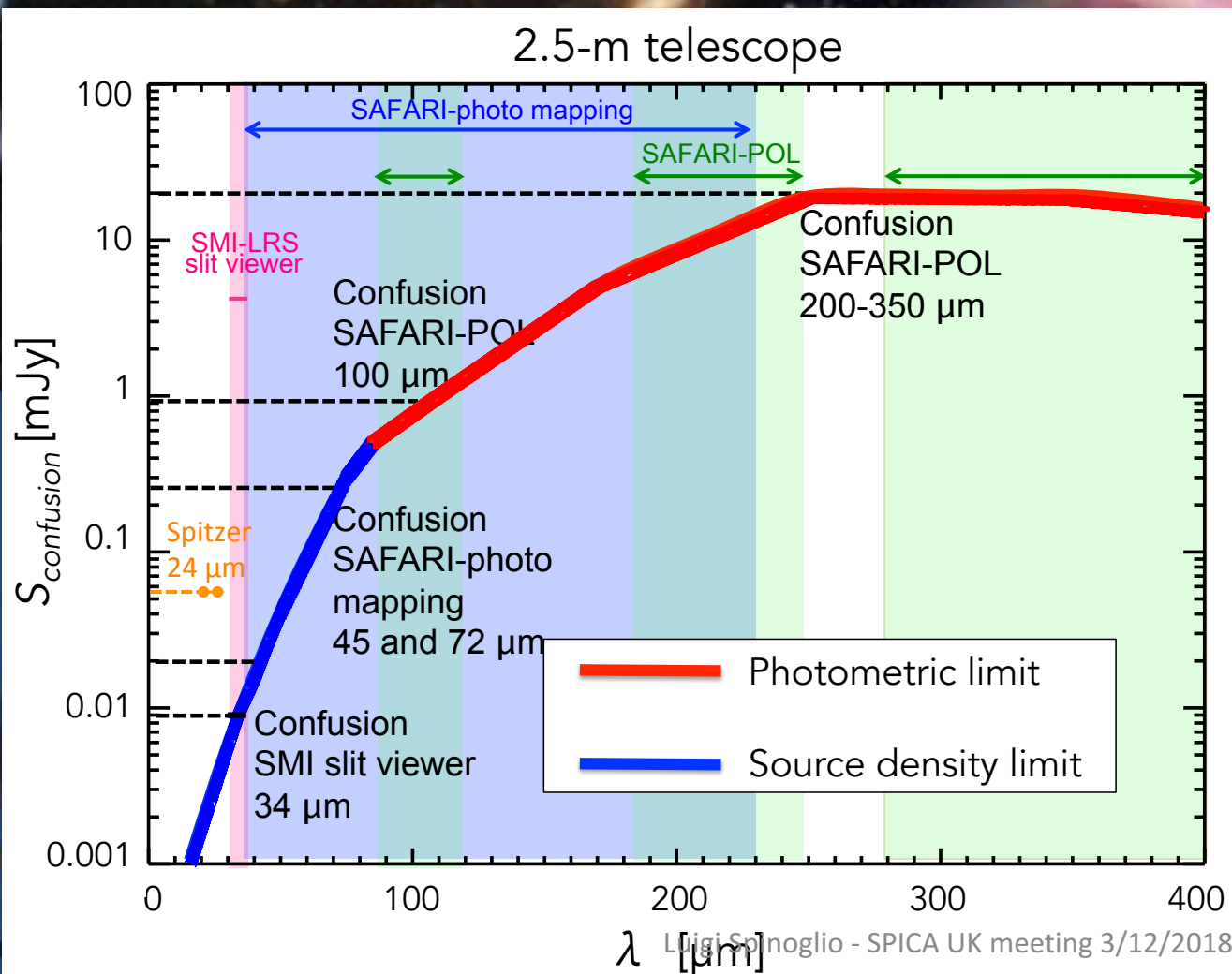
SPICA SMI deep surveys will detect AGN and starburst galaxies up to $z \sim 5-6$, characterized by SPICA spectral follow-up + ELTs and ALMA



Left: $L-z$ plane coverage of a 0.2 deg^2 SMI survey at the confusion limit ($5 \mu\text{Jy}$, 10 hours/frame).
Right: The SED fit to the $z=4.3$ starburst galaxy GN20 (Efstathiou & Siebenmorgen 2009) rescaled to $L=10^{12} L_{\odot}$ for $z=3-6$. The detection limits of ALMA (10 minutes), ELT/MOS and ELT/ MICADO (3 hours) are shown. SPICA will map large areas to the confusion limit one hundred times faster than JWST, finding large numbers of dust-enshrouded AGN and starbursts at $z > 5$.

A photometric survey with SPICA

1. SMI/CAM 34 μ m or
 2. SMI/CAM 34 μ m+ B-POL@60-70 μ m [34-60] or [34-70] colors
- explore the sensitivity with the confusion limit at these bands



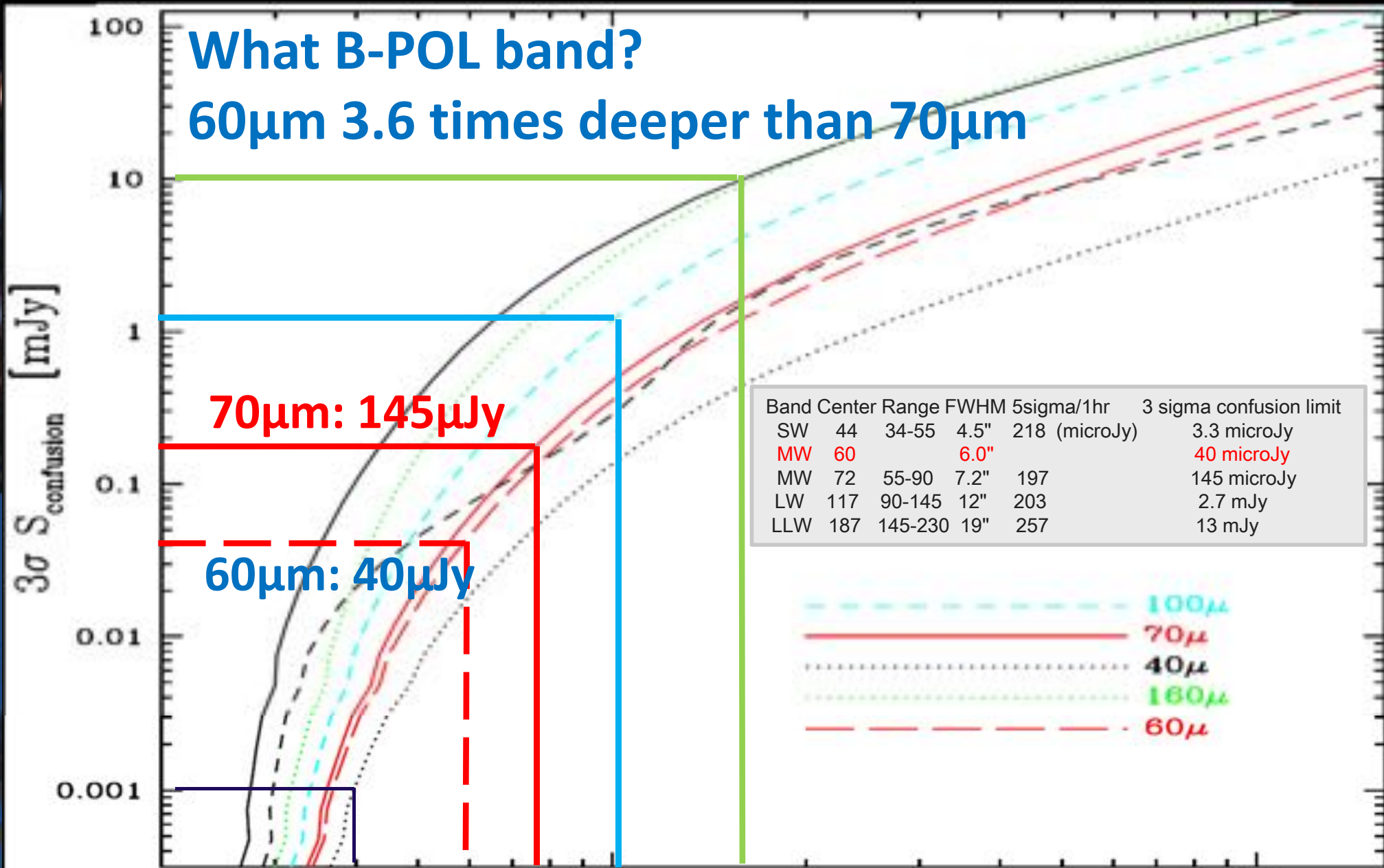
Confusion limit for a diffraction-limited 2.5-m telescope. The blue curve is determined by the source density criterion, while the red one is defined by the photometric criterion.

The 5σ -confusion of SMI/CAM (34 μ m) is 9 μ Jy, the SAFARI confusion is 0.02, 0.25 and 1 mJy at 45, 72 and 100 μ m, and 18 mJy at > 200 μ m.

3 σ confusion limits for a 2.5 m SPICA telescope

What B-POL band?

60 μ m 3.6 times deeper than 70 μ m



Luigi Spinoglio - SPICA UK meeting 3/12/2018

PSF FWHM θ_0 (arcsec)

A photometric survey with “only” SPICA SMI/CAM

Survey Strategy

White paper by Carlotta Gruppioni et al. (2017, PASA)

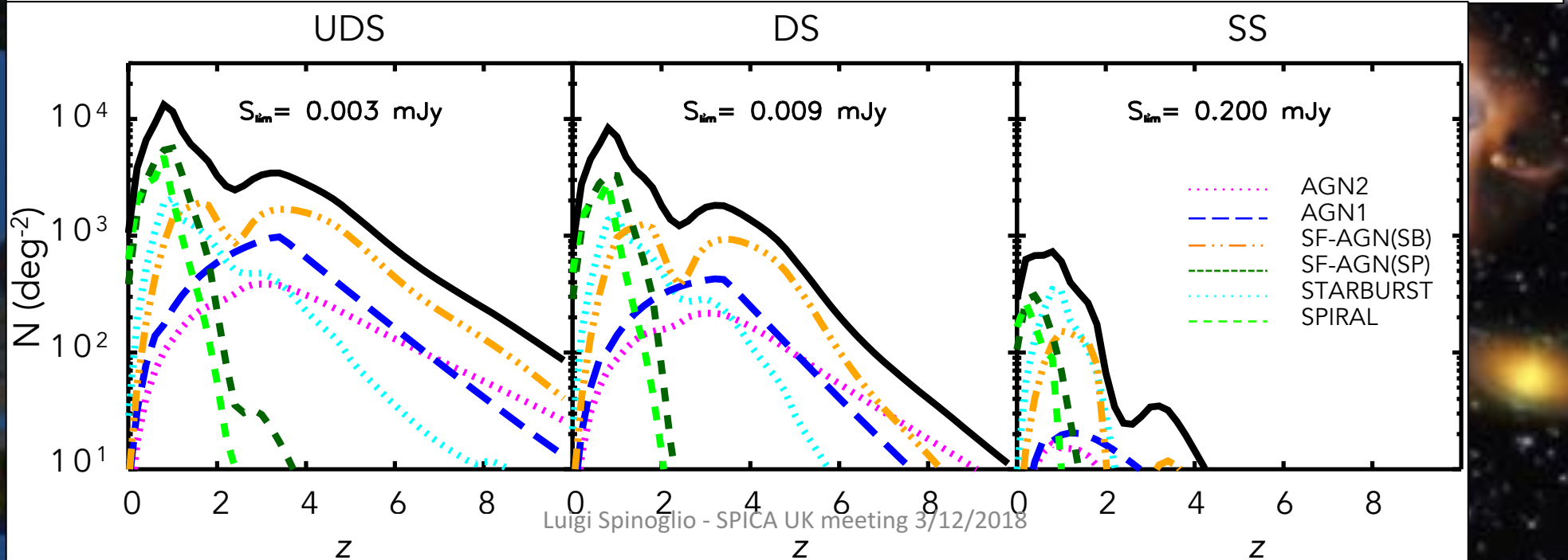
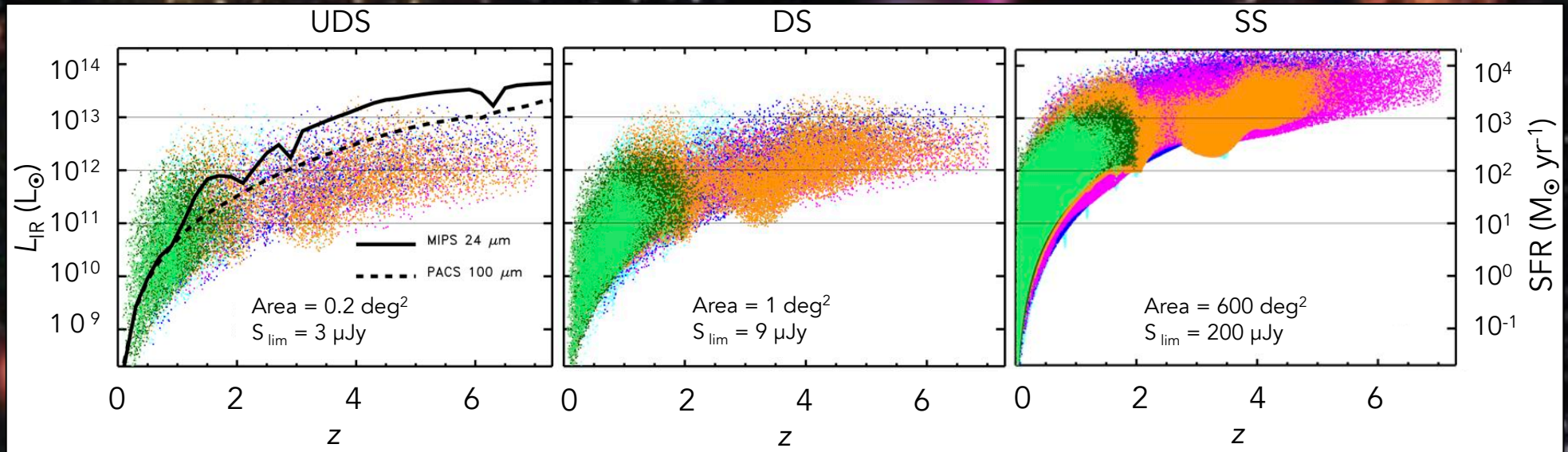


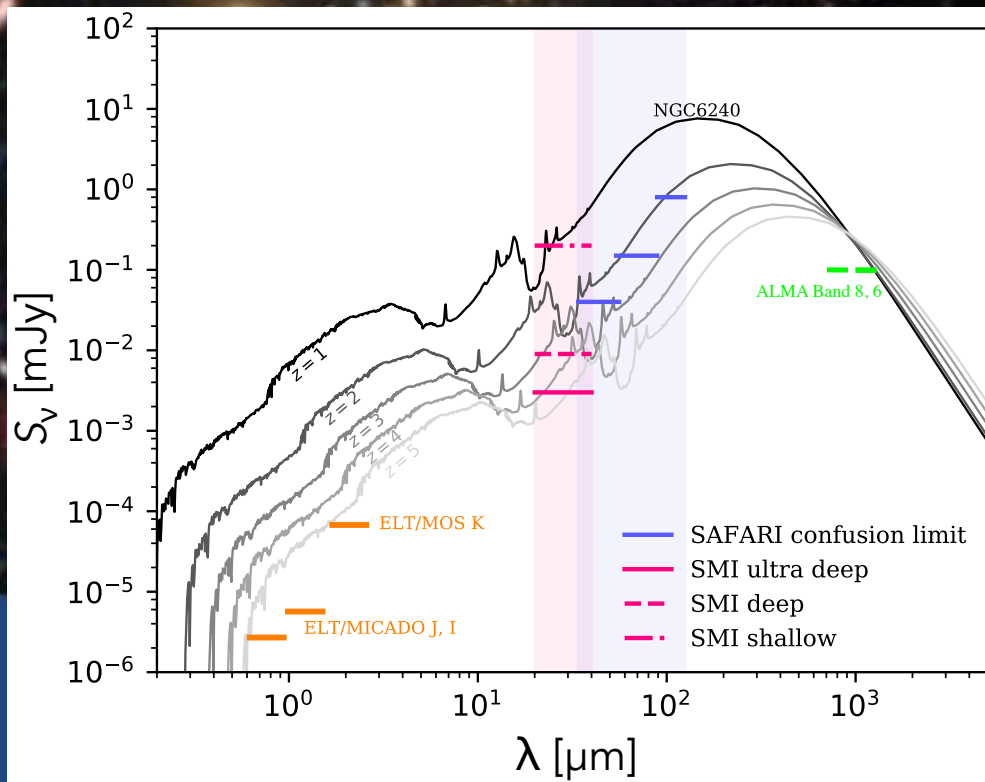
Table 1 Expected No. of sources in the SMI 34- μm survey.

z	No. UDS Tot (AGN)	No. DS Tot (AGN)	No. SS Tot (AGN)
0–1	6.3 (3.0) $\times 10^3$	2.1 (0.9) $\times 10^4$	1.7 (0.8) $\times 10^6$
1–2	7.3 (4.9) $\times 10^3$	2.2 (1.5) $\times 10^4$	1.4 (0.5) $\times 10^6$
2–3	2.7 (2.2) $\times 10^3$	7.1 (5.4) $\times 10^3$	1.4 (0.8) $\times 10^5$
3–4	3.2 (2.9) $\times 10^3$	8.4 (7.3) $\times 10^3$	9.0 (7.2) $\times 10^4$
4–5	2.3 (2.1) $\times 10^3$	5.2 (4.9) $\times 10^3$	2.5 (2.4) $\times 10^4$
5–6	1.2 (1.1) $\times 10^3$	1.9 (1.9) $\times 10^3$	4.1 (4.1) $\times 10^3$
6–7	5.6 (5.5) $\times 10^2$	5.7 (5.7) $\times 10^2$	9.0 (9.0) $\times 10^2$
>7	1.2 (1.2) $\times 10^1$	8.0 (8.0) $\times 10^0$	1.8 (1.8) $\times 10^1$

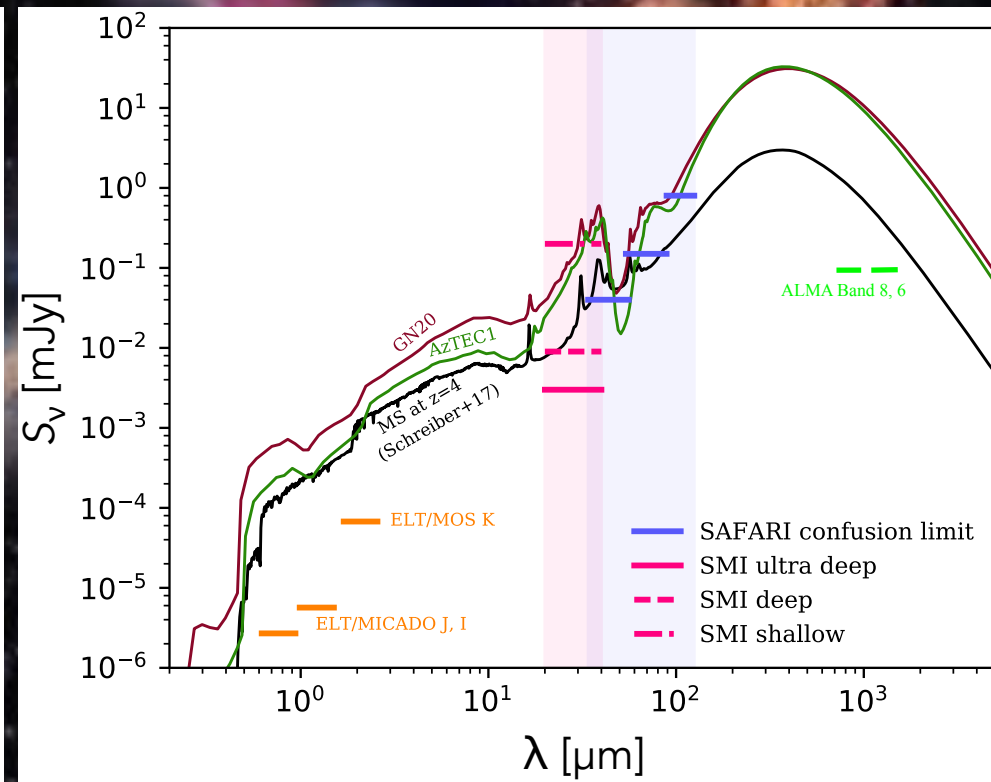
White paper by Carlotta Gruppioni et al. (2017, PASA)



HOW TO CONSTRAIN THE SEDs OF SMI FAINT GALAXIES



Template SED of the local CT AGN scaled by redshift up to $z=5$.



Fits to the observed SEDs of: the $z \approx 4$ starburst galaxy GN20 (purple) and the $z=4.34$ sub-mm galaxy AzTEC-1 (green).

White paper by Carlotta Gruppioni et al. (2017, PASA)

From the science goals to the reference mission definition

2.1.1 Star formation and Black Hole accretion

- | | | | |
|--|---|---|--------------------|
| 1. High-res MIR spectroscopy:
Spatial coverage: ~1000 pointings | $\lambda\lambda = 17-36\mu\text{m}$
Line Sensitivity: $5 \times 10^{-20} \text{ Wm}^{-2} [5\sigma]$ | $R \sim 1300-2200$ | T.=1300 hrs |
| 2. Medium-res FIR spectroscopy:
Spatial coverage: ~1000 pointings | $\lambda\lambda = 35-230\mu\text{m}$ {Goal: 35-320 μm }
Line Sensitivity: $5 \times 10^{-20} \text{ Wm}^{-2} [5\sigma]$ | $R \sim 300$ | T.=1300 hrs |
| 3. Low-res MIR spectroscopy:
Spatial cov.: $0.2^\circ \times 0.17^\circ$ (1 x 10' x 12' frame)
+ Wide-band MIR imaging:
Spatial cov.: $0.2^\circ \times 0.17^\circ$ (1 x 10' x 12' frame) | $\lambda\lambda = 17-36\mu\text{m}$
ULTRA-DEEP Line Sens.: $\sim 2 \times 10^{-20} \text{ Wm}^{-2} [5\sigma]$
$\lambda\lambda = 17-36\mu\text{m}$
ULTRA-DEEP Cont. Sens.: $< 3 \mu\text{Jy} [5\sigma]$ below confusion | $R \sim 50-120$
$R \sim 5$ Ang. Res.: $\sim 3''$ | T.= 19 hrs |
| 5. Low-res MIR spectroscopy:
Spatial cov.: $1^\circ \times 1^\circ$ (spread over several patches)
+ Wide-band MIR imaging:
Spatial cov.: $1^\circ \times 1^\circ$ (spread over several patches) | $\lambda\lambda = 17-36\mu\text{m}$
DEEP Line Sensitivity: $3 \times 10^{-20} \text{ Wm}^{-2} [5\sigma]$
$\lambda \sim 34 \mu\text{m}$ {Goal: 27 μm }
DEEP Sens.: $< 5 \mu\text{Jy} [5\sigma]$ to achieve confusion | $R \sim 50-120$
$R \sim 5$ Ang. res.: $\sim 3''$ | T.=203 hrs |
| 7. Wide-band FIR imaging:
Spatial cov.: $0.2^\circ \times 0.17^\circ$ (1 x 10' x 12' frame) | $\lambda \sim 60 \mu\text{m}$
ULTRA-DEEP Cont. Sens.: $< 15 \mu\text{Jy} [5\sigma]$ below confusion | $R \sim 5$ Ang. res.: $\sim 6''$ | T.=19 hrs |
| 8. Wide-band FIR imaging:
Spatial cov.: $1^\circ \times 1^\circ$ (spread over several patches) | $\lambda \sim 60 \mu\text{m}$
DEEP $< 30 \mu\text{Jy} [5\sigma]$ to achieve confusion-limit | $R \sim 5$ Ang. res.: $\sim 6''$ | T.=138 hrs |

2.1.2 Feeding and feedback in galaxies

High-res FIR spectroscopy $\lambda\lambda=35-230\mu\text{m}$ {Goal: 35-320 μm } R~1800-12000 **T.=480 hrs**
Spatial coverage: ~120 pointings Sensitivity: $1 \times 10^{-19} \text{ Wm}^{-2}$ [5 σ] {Goal: $6 \times 10^{-20} \text{ Wm}^{-2}$ [5 σ]}

2.1.3 The rise of metals and dust

Very High-res MIR spectroscopy: $\lambda\lambda=12-18\mu\text{m}$ R~28000 (Pf α at $z \sim 1$) **T.=250 hrs**
Spatial coverage: ~360 pointings Sensitivity: $\sim 2 \times 10^{-20} \text{ Wm}^{-2}$ [5 σ]

2.1.4 Detecting Early Black Holes and Starbursts

1. Wide-band MIR imaging photometry: $\lambda\lambda=34\mu\text{m}$ R~5 **T.=79 hrs**
Spatial cov.: 625 deg² (**SHALLOW**) (spread over several patches) Sensitivity: 0.2 mJy [5 σ]
Or
Spatial cov.: 100 deg² (**SHALLOW**) (spread over several patches) Sensitivity: 0.08 mJy [5 σ]

2. Wide-band FIR imaging photometry: $\lambda\lambda=60\mu\text{m}$ R~5 **T.=138 hrs**
Spatial cov.: 625 deg² (**SHALLOW**) (spread over several patches) Sensitivity: 0.75 mJy [5 σ]
Or
Spatial cov.: 100 deg² (**SHALLOW**) (spread over several patches) Sensitivity: 0.30 mJy [5 σ]

2.1.5 Characterizing Early Black Holes and Starburst Galaxies

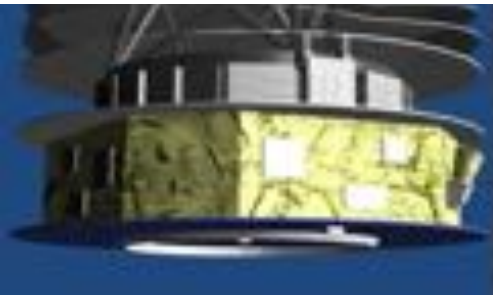
1. Medium-res FIR spectroscopy: $\lambda\lambda=35-230\mu\text{m}$ R~300 **T.=500 hrs**
Spatial coverage: ~50 pointings Sensitivity: $5 \times 10^{-20} \text{ Wm}^{-2}$ [5 σ] {Goal: $3 \times 10^{-20} \text{ Wm}^{-2}$ [5 σ]}

2.1.6 Physics of the ISM and activity in Local galaxies

- | | | | |
|---|--|---|-------------------|
| 1. High-res FIR spectroscopy
Spatial coverage: ~600 pointings | $\lambda\lambda = 35-230\mu\text{m}$ {Goal: 35-320 μm }
Sensitivity: $1 \times 10^{-19} \text{ Wm}^{-2}$ [5σ] {Goal: $6 \times 10^{-20} \text{ Wm}^{-2}$ [5σ]} | $R \sim 1800-12000$ | T.=300 hrs |
| 2. High-res MIR spectroscopy:
Spatial coverage: ~600 pointings | $\lambda\lambda = 17-36\mu\text{m}$
Sensitivity: $\sim 5 \times 10^{-20} \text{ Wm}^{-2}$ [5σ] | $R \sim 1300-2200$ | T.=20 hrs |
| 3. Very High-res MIR spectroscopy:
Spatial coverage: ~360 pointings | $\lambda\lambda = 12-18\mu\text{m}$
Sensitivity: $\sim 2 \times 10^{-20} \text{ Wm}^{-2}$ [5σ] | $R \sim 28000$ (Pf α at $z \sim 1$) | T.=20 hrs |
| 4. Medium-res FIR spectroscopy:
Spatial coverage: ~40 pointings (for HD detection) | $\lambda\lambda = 35-230\mu\text{m}$
Sensitivity: $5 \times 10^{-20} \text{ Wm}^{-2}$ [5σ] | $R \sim 300$ | T.=40 hrs |

2.1.7 Nearby (resolved) galaxies

- | | | | |
|--|--|---|-------------------|
| 1. Medium-res Imaging FIR spectroscopy:
Spatial coverage: ~20 pointings, 10'x7' coverage | $\lambda\lambda = 35-230\mu\text{m}$
Sensitivity: $1 \times 10^{-18} \text{ Wm}^{-2}$ [5σ] | $R \sim 300$ | T.=200 hrs |
| 2. High-res Imaging MIR and FIR spectroscopy:
Spatial coverage: 20 pointings, 1'x1' to 10'x10' coverage (TBC) | $\lambda\lambda = 17-230\mu\text{m}$
Sens.: $50 \times 10^{-20} \text{ Wm}^{-2}$ [5σ] | $R \sim 1500$ | |
| 3. Imaging FIR polarimetry:
Spatial coverage: ~50 sources @10'x10' | $\lambda\lambda = 75-420 \mu\text{m}$
Sensitivity: 1 MJy/sr [5% pol fraction, 5σ] | $R \sim 2$ Angular res.: $\sim 10''$ FWHM @ 100 μm | |



Mode		Science cases	Type of obs	Resolution	No. srcs	FOV/src	Integ time (hrs)
MIR spectroscopy	Low-res	2.1.1	Stare-step	Diff	1	0.2°x0.17°	19
		2.1.1	Stare-step	Diff	1	1.0°x1.0°	203
		2.1.4	Stare-step	Diff	1	n/a	2.1.1
	High-res	2.1.1	Stare	Diff	1000	n/a	1300
		2.1.2	Stare	Diff	500	n/a	2.1.1
		2.1.3	Stare	Diff	1000	n/a	2.1.1
		2.1.6	Stare	Diff	600	n/a	75
		2.1.7	Stare-step	2 @ 20	20	1'-10' ^2	?
	Very-high-res	2.1.3	Stare	2 @ 20	360	n/a	250
		2.1.6	Stare	2 @ 20	600	n/a	20
MIR imaging photometry	Wide-band	2.1.1	Stare-step	3 @ 30	1	0.2°x0.17°	2.1.1LR
		2.1.1	Stare-step	3 @ 30	1	1.0°x1.0°	2.1.1LR
		2.1.3	Stare	2 @ 20	1000	n/a	2.1.3MR
		2.1.4	Stare-step	3 @ 30	1	1.0°x1.0°	2.1.1LR
		2.1.4	Stare-step	3 @ 30	1	25°x25°/10°x10°	79
FIR spectroscopy	Medium-res	2.1.1	Stare	Diff	1000		1300
		2.1.2	Stare	Diff	500	n/a	2.1.1
		2.1.3	Stare	Diff	1000	n/a	2.1.1
		2.1.5	Stare	Diff	50		500
		2.1.6	Stare	Diff	40	n/a	40
		2.1.7	Stare-step	Diff	20	10'x7'	200
		High-res	2.1.2	Stare	Diff	120	n/a
2.1.6	Stare		Diff	600	n/a	300	
2.1.7	Stare-step		Diff	20	<10' ^2	?	
FIR imaging photometry	Wide-band	2.1.1	OTF	Diff	1	0.2°x0.17°	19
		2.1.1	OTF	Diff	1	1.0°x1.0°	138
		2.1.4	OTF	Diff	1	1.0°x1.0°	2.1.1
		2.1.4	OTF	Diff	1	25°x25°/10°x10°	140

